

The Nevado del Huila Volcanic Complex

<https://doi.org/10.32685/pub.esp.38.2019.06>

Published online 1 October 2020

Ana María CORREA-TAMAYO^{1*} , Bernardo Alonso PULGARÍN-ALZATE² ,
and Eumenio ANCOCHEA-SOTO³ 

Abstract The Nevado del Huila Volcanic Complex, so named since 1995, is the tallest active volcano (5364 masl) in Colombia. Its eruptive history, which began at 1.5 Ma (early Pleistocene), is divided into three stages: the Pre-Huila Stage, which ended 100 000 years ago; the Ancient Huila Stage (Late Pleistocene), which continued until the end of the Last Glaciation; and the Recent Huila Stage, which began 11 000–10 000 years ago (Holocene). These stages led to the construction of two main volcanic edifices (Pre-Huila and Huila). Thirteen volcano-stratigraphic units have been defined. They are predominantly lava flow accumulations, and the most recent product is an assemblage of domes located at the summit. This apparently monotonous depositional history was significantly interrupted in the Late Pleistocene by gravitational collapse of the southern flank, generating a large debris avalanche and associated debris flows. The most recent eruptions, between 2007 and 2010, culminated in the extrusion of a new dome and the formation of several lahars, one of which was larger than the 1985 lahar at the Nevado del Ruiz Volcano that buried the town of Armero. The eruptive history of the Nevado del Huila Volcanic Complex is the result of equally complex magmatic evolution, which is reflected in the geomorphological variability and the textural and geochemical diversity of its products. Based on these variations and on the ⁸⁷Sr/⁸⁶Sr and ¹⁴³Nd/¹⁴⁴Nd isotope ratios, we suggest that magmatic petrogenesis was mainly controlled by partial melting of a metasomatized mantle wedge and that magmatic differentiation was mainly due to fractional crystallization in a subduction environment associated with an active continental margin.

Keywords: *Nevado del Huila, Pleistocene – Holocene, andesite, dacite, Colombia.*

Resumen El Complejo Volcánico Nevado del Huila, denominado así desde 1995, es el volcán activo más alto (5364 m s. n. m.) de Colombia. Su historia eruptiva, que comenzó hace 1,5 Ma (Pleistoceno temprano), se divide en tres estadios: Estadio Pre-Huila, que terminó hace 100 000 años; Estadio Huila Antiguo (Pleistoceno Tardío), que continuó hasta finales de la Última Glaciación; y Estadio Huila Reciente, que comenzó hace 11 000–10 000 años (Holoceno). Estos estadios conllevaron a la construcción de dos edificios volcánicos principales (Pre-Huila y Huila). Se han definido trece unidades volcanoestratigráficas. Son predominantemente acumulaciones de flujos de lavas, y el producto más reciente es un conjunto de domos ubicado en su cima. Esta historia de depósito aparentemente monótona se vio interrumpida drásticamente en el Pleistoceno Tardío por el colapso gravitacional del flanco sur, que generó una enorme avalancha de escombros y flujos de escombros asociados. Las erupciones más recientes, entre 2007 y 2010, culminaron con la extrusión de un nuevo domo y la formación de varios

- 1 acorrea@sgc.gov.co
Servicio Geológico Colombiano
Dirección de Geociencias Básicas
Diagonal 53 n.º 34–53
Bogotá, Colombia
 - 2 bpulgarin@sgc.gov.co
Servicio Geológico Colombiano
Dirección de Geociencias Básicas
Observatorio Vulcanológico y Sismológico
de Popayán
Calle 5B n.º 2–14
Popayán, Cauca, Colombia
 - 3 anco@ucm.es
Universidad Complutense de Madrid
Facultad de Ciencias Geológicas
28040 Madrid, España
- * Corresponding author

Supplementary Information:

S: <https://www2.sgc.gov.co/LibroGeologiaColombia/tgc/sgcpubesp38201906s.pdf>

Citation: Correa-Tamayo, A.M., Pulgarín-Alzate, B.A. & Ancochea-Soto, E. 2020. The Nevado del Huila Volcanic Complex. In: Gómez, J. & Pinilla-Pachon, A.O. (editors), *The Geology of Colombia, Volume 4 Quaternary. Servicio Geológico Colombiano, Publicaciones Geológicas Especiales 38*, p. 227–265. Bogotá. <https://doi.org/10.32685/pub.esp.38.2019.06>

lahares, uno de ellos de magnitud superior al ocurrido en 1985 en el Volcán Nevado del Ruiz que enterró a la población de Armero. La historia eruptiva del Complejo Volcánico Nevado del Huila es el resultado de una evolución magmática igualmente compleja, reflejada en la variedad geomorfológica y la diversidad textural y geoquímica de sus productos. Con base en estas variaciones y en las relaciones isotópicas $^{87}\text{Sr}/^{86}\text{Sr}$ y $^{143}\text{Nd}/^{144}\text{Nd}$ se sugiere que la petrogénesis magmática fue controlada principalmente por la fusión parcial de una cuña mantélica metasomatizada y esa diferenciación magmática se debió principalmente a la cristalización fraccionada en un ambiente de subducción asociado a un margen continental activo.

Palabras clave: Nevado del Huila, Pleistoceno–Holoceno, andesita, dacita, Colombia.

1. Introduction

The Nevado del Huila Volcano is located between the Cauca, Huila, and Tolima Departments (Figure 1), within the Parque Nacional Natural Nevado del Huila. It is in the highest part of the Central Cordillera and is the highest active volcano (5364 masl) in Colombia. The nearest town is the municipality of Belalcázar (Cauca Department, located 30 km SSE from its summit. It is considered to be an active volcano due to its continuous seismic activity, the presence of hot springs, continuous fumarolic activity, and geological evidence of Holocene pyroclastic density currents. Its activity was demonstrated by eruptions between 2007 and 2010, which were associated with significant seismic activity, changes in glacial mass, abundant fumarolic activity associated with large cracks, enormous lahars, ash fall, and the emplacement of a new dome at the summit. Since 1992, the Servicio Geológico Colombiano, through the Observatorio Vulcanológico y Sismológico de Popayán, has been responsible for the surveillance and monitoring of this volcano.

Before 1994, there was little information about the Nevado del Huila. This situation changed after a magnitude 6.4 earthquake that occurred on 6 June 1994, whose epicenter was at the base of the southwestern slope. Although this earthquake was not associated with volcanic activity, it aroused great concerns about the eventual reactivation of the volcano and led to new volcanic studies, which included characterization of deposits, a stratigraphic survey, geological mapping, and geochronological studies to better understand the volcano eruptive history. These results were used to prepare a proper volcanic hazard map. These studies were supplemented with additional research that expanded the geological knowledge of this volcano. Recently, several $^{40}\text{Ar}/^{39}\text{Ar}$ dates were obtained to complement the age range that frames its eruptive history.

1.1. Previous Studies

Before 1995 (e.g., Forero, 1956; Hantke & Parodi, 1966; Ramírez, 1968; Simkin, 1981), this volcano was considered a stratovolcano with mainly effusive activity, and it was measured at 5750 masl. Since then, based on geomorphological analysis

and geological studies, it has become known as the Nevado del Huila Volcanic Complex (NHVC).

Since the end of the 19th century, several authors have performed geological, morphological, glaciological, volcanic hazard, and historical activity studies. Stübel (1906) was the first to indicate that the NHVC is composed of augite andesites and dacites. Cepeda et al. (1986) performed a general geological survey of the volcano and prepared the “Mapa de riesgos volcánicos potenciales del Nevado del Huila – Map of potential volcanic risks of the Nevado del Huila”. Later, Flórez (1990) and Flórez & Ochoa (1990) performed photogrammetric studies on glacial retreat at Nevado del Huila. Espinosa (2001), in his work on historical eruptions of Colombian volcanoes, noted that Nevado del Huila was identified by Spanish conquerors as a volcano in 1550.

After the Páez earthquake of 6 June 1994, several studies were carried out regarding its characteristics and the effects it produced (e.g., Caro, 1995; Caro & Ruge, 1997; Jiménez, 1997), together with other studies related to associated volcanic hazards (e.g., Ingeominas, 1995a). Several geological and geomorphological studies were performed, the most notable of which are the studies by Correa-Tamayo & Cepeda (1995) and Cepeda et al. (1997), who classified the area as a volcanic complex. Later, other studies provided more detailed information on geomorphological, geological, stratigraphic, and petrographic aspects (e.g., Correa-Tamayo & Pulgarín, 2002; Correa-Tamayo et al., 2000; Pulgarín & Correa-Tamayo, 1997, 2001; Pulgarín et al., 1997a, 1997b).

Pulgarín et al. (1996, 2007) analyzed glacial retreat on Nevado del Huila between 1961 and 1995 by means of analytical photogrammetry and demonstrated an areal loss of 5.47 km² (29%) and a volumetric loss of 0.27 km³. Subsequently, correlations between the identified moraines and other glaciated areas of Colombia were performed (Pulgarín & Correa-Tamayo, 2003). Ariza (2006) also calculated the change in glacial area between 1976 and 2001 using Landsat images, obtaining an areal loss of 27%.

Pulgarín (2000) and Pulgarín et al. (2004) identified a succession of Upper Pleistocene debris avalanche and debris flow deposits along the banks of the Páez River south of the vol-

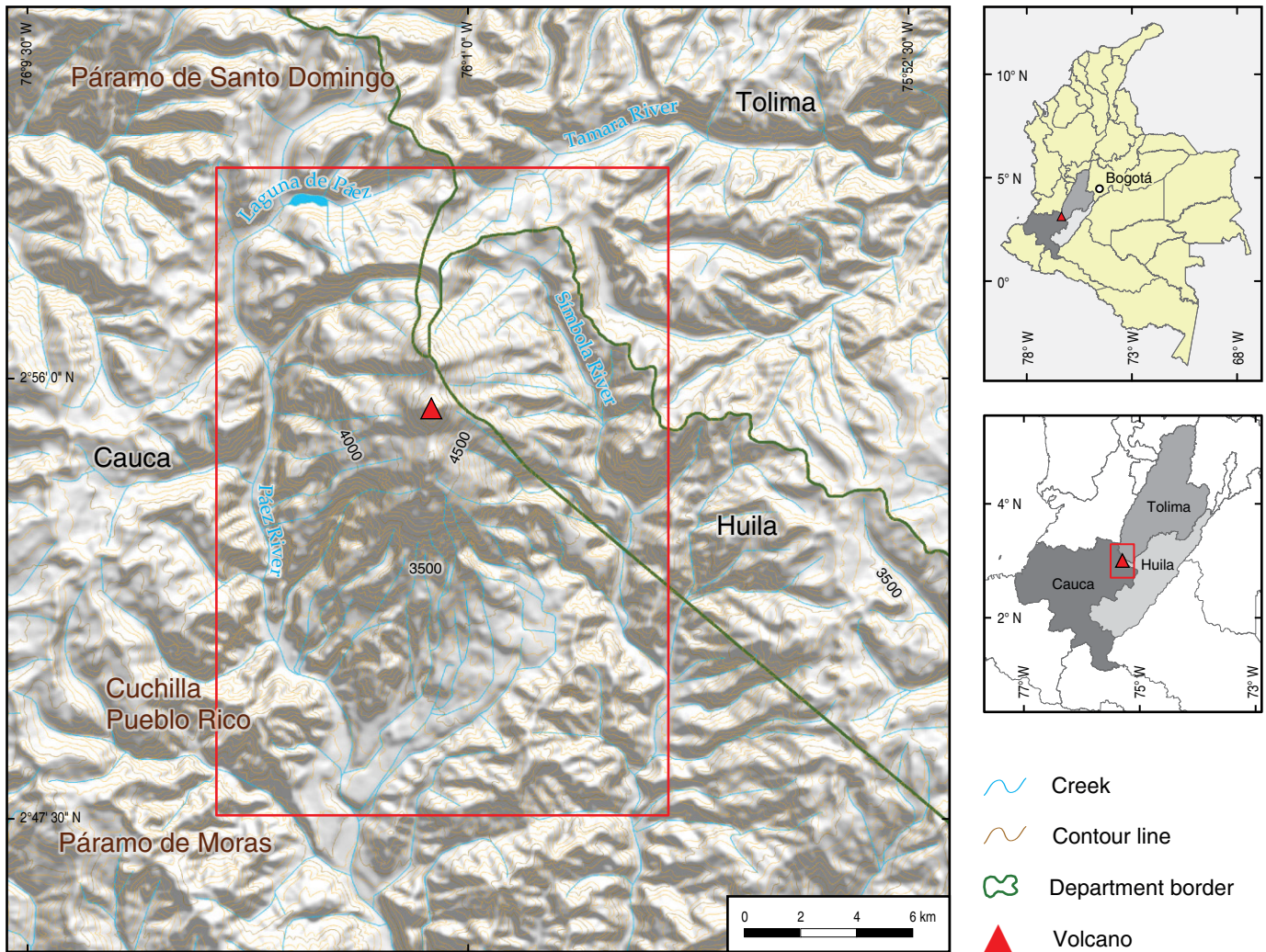


Figure 1. Location map of the Nevado del Huila Volcanic Complex in Colombia.

cano, which are associated with the gravitational collapse of the southern flank of the NHVC. Pulgarín (2003) developed a flood map by modeling debris flows along the Páez River valley following the methodology in Iverson et al. (1998).

An investigation of the petrology, geochemistry, and mineral chemistry of the lava products of the NHVC, supported by isotopic dating (whole-rock K–Ar), performed by Correa–Tamayo (2009), established the petrogenetic processes that determined its magmatic evolution. The results of this research were partially published by Correa–Tamayo et al. (2011) and Correa–Tamayo & Ancochea (2015a, 2015b) and more fully in this chapter, which is the first time that an integral synthesis of these results together with the results of other research related to the NHVC and new unpublished isotopic dates ($^{40}\text{Ar}/^{39}\text{Ar}$), have been formally published in an international medium.

After the NHVC reactivation in 2007, different geological studies were performed that characterized the surface changes caused by the eruptions of 2007 and 2008, as well as the various events that it generated: lahars, ash falls, extrusion of the new

dome, and morphological changes in the glacial mass (Manzo et al., 2011; Monsalve et al., 2011; Pulgarín, 2012; Pulgarín et al., 2008, 2009, 2015). Additionally, seismological studies were carried out, in which the seismic events associated with three eruptions that occurred between 2007 and 2008 and the entire eruptive process up to 2010 were described (Cardona et al., 2009; Londoño & Cardona, 2011; Santacoloma et al., 2009). Later, Pulgarín & Laverde (2015a) correlated the events of ash emissions and seismic events associated with the 2007–2010 activity with the respective ash dispersion events reported by the Volcanic Ash Advisory Center of Washington; this correlation served to update the hazard map due to pyroclastic fallout (Pulgarín & Laverde, 2015b).

1.2. Geological Setting

The NHVC is one Colombian active volcano located in the North Volcanic Zone (NVZ) of the Andes and is the result of subduction of the Nazca Plate under the South American Plate

in the NW corner of South America (Alvarado *et al.*, 1999; Arcila *et al.*, 2000; Jaillard *et al.*, 2002; Taboada *et al.*, 2000). Since the Mesozoic, when the North Andean Block (the Andes of Colombia) was formed, it has been subjected to compression and collision forces, combined with localized extension evidenced by volcanism (Meissner *et al.*, 1980).

The NHVC is located in the Central Cordillera of the Northern Andes, separated from the other groups of volcanoes that constitute the Colombian volcanic chain by zones in which there is no volcanism; these variations are attributed to changes in the inclination of the subducted plate (Hall & Wood, 1985), at the site where longitudinal NE–SW faults (*i.e.*, Moras Fault System) intersect with NW–SE transverse faults. The eruptive history of the NHVC is framed within the second stage of Colombian Cenozoic volcanism, which spans the late Pliocene to the Holocene (Cepeda, 1987; Cepeda *et al.*, 1987; Toussaint & Restrepo, 1991). This volcanism developed in an arc, formed at an active continental margin located 200 km from the Colombia–Ecuador Trench, 150 km above the Benioff zone (Meissner *et al.*, 1980). Its basement (Figure 2) consists of Paleozoic metamorphic rocks, the Quintero Gneiss (Pznq) and Cajamarca Complex (Pzmc); Mesozoic intrusive rocks, La Plata Batholith (J?bp); Cretaceous metasedimentary and sedimentary rocks (Kms); and Tertiary intrusive rocks (T?i).

2. Samples and Methods

Previously, a detailed geomorphological analysis was carried out using 50 aerial photographs taken in 1995 along five flight lines (R1194, from Instituto Geográfico Agustín Codazzi) in a N–S direction at scales between 1:23 000 and 1:29 000 and subsequent cartographic and stratigraphic surveys in five field expeditions. Based on the volcano stratigraphic survey and the detailed geomorphological analysis, the eruptive history of the NHVC was reconstructed (Pulgarín *et al.*, 1997b), and the corresponding geological map was prepared at a scale of 1:25 000. In the geomorphological analysis, several parameters were considered: height above sea level, slope, surface features in aerial imagery, drainage pattern, sizes of the geofoms, degree of erosion, shapes and sizes of escarpments, vegetal cover, degree of incision, and superposition among volcanic geofoms.

Moraines were mapped to define the different glacial stages that have affected the NHVC. Using aerial photos and field information, the lower elevations of the lateral moraine fronts were inventoried. A total of 123 data points were obtained between the lowest elevation (2650 masl) and the highest (4550 masl). Then, an altimetric correlation was made with moraines from glacial stages recognized in other glacial zones of Colombia (Central Cordillera, Sierra Nevada de Santa Marta, Sierra Nevada del Cocuy, páramo de Sumapaz, and the Bogotá Altiplano).

From the 216 lava samples collected (see Table 1 of the Supplementary Information), 51 representative samples were

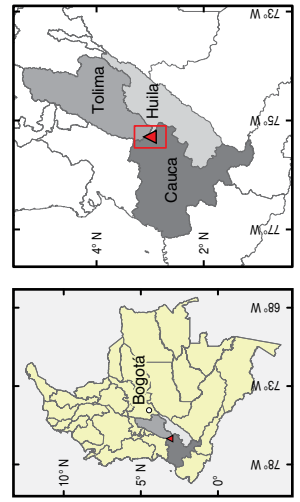
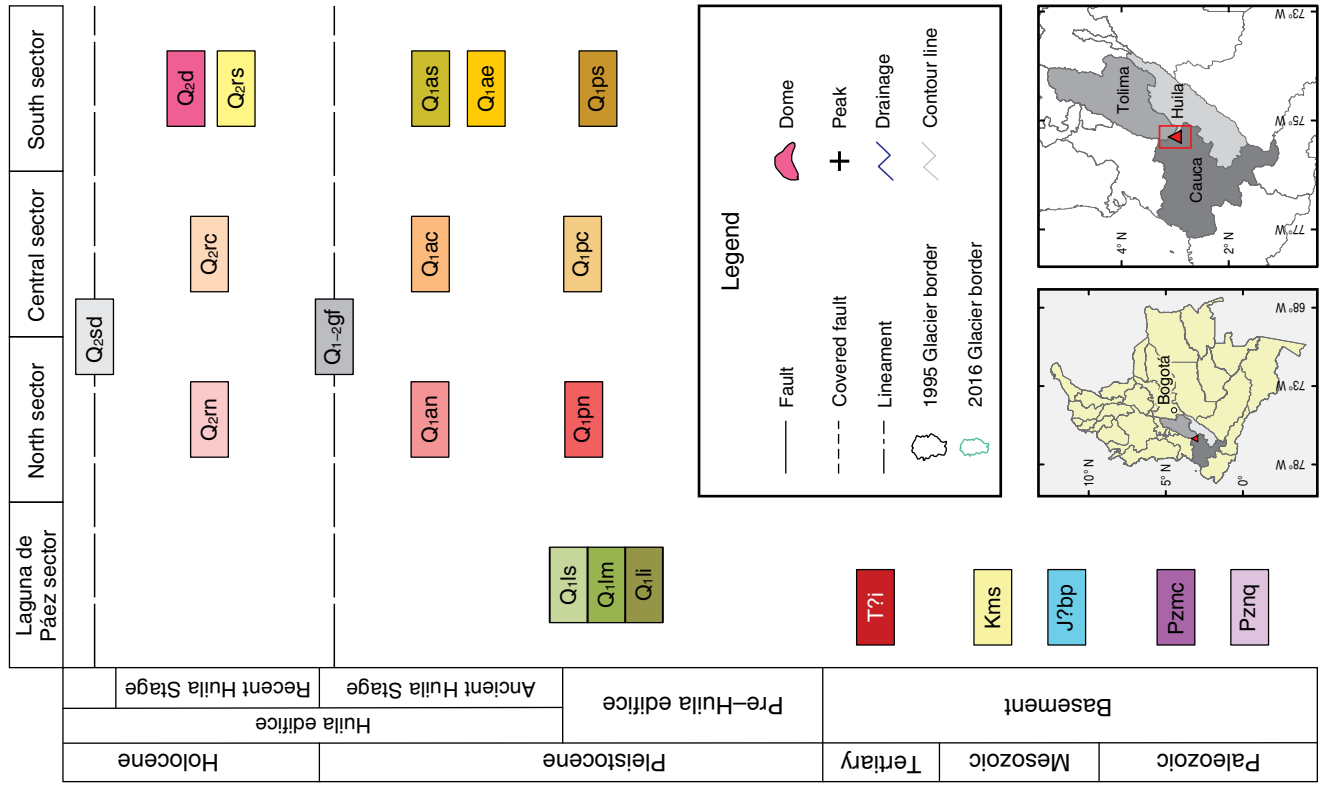
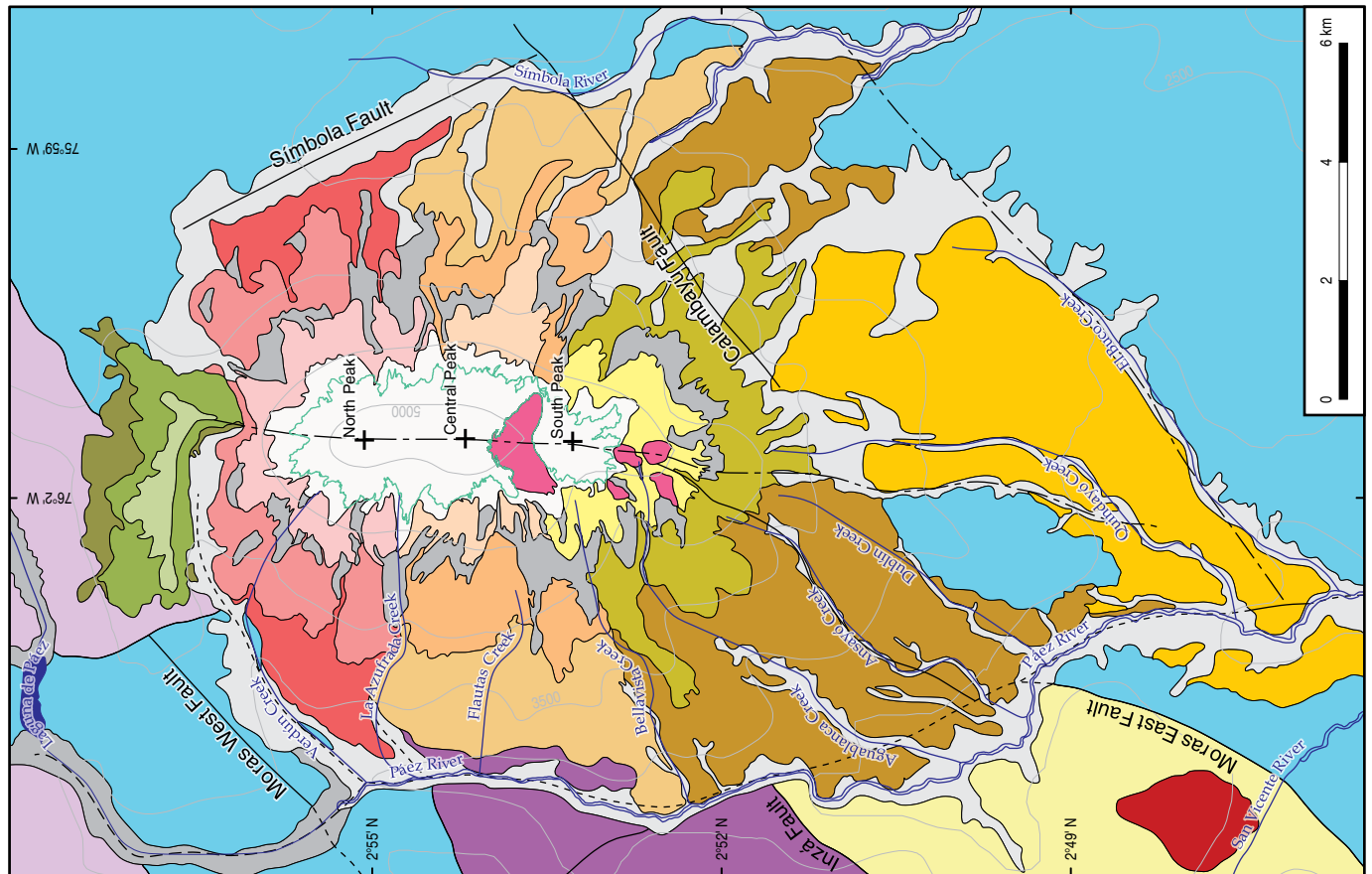
sent to Actlabs Laboratories (Canada) for whole-rock chemical analyses (see Tables 2, 3, 4, and 5 of the Supplementary Information). Major and selected trace elements were analyzed with ICP (inductively coupled plasma) emission spectroscopy, and most trace elements, including REEs (rare earth elements), with ICP–MS (inductively coupled plasma mass spectrometry). As part of the initial processing of the data, the concentration values of major elements were recalculated at 100% anhydrous conditions. Both Fe₂O₃ and FeO were recalculated according to Le Maitre's (1976) equations for volcanic rocks.

For the petrographic characterization of lava samples, the following characteristics were considered: mineralogical composition, texture of the rock, characteristics of the matrix, types of phenocrysts, special textural features, modal percentages of each mineral and of each size category, and specific characteristics of each mineral phase. The petrographic classification was based on modal percentages (% volume) recalculated to 100% of each mineral phase present in 201 thin sections analyzed, from phenocryst size (size > 2 mm) to microphenocrysts (2 to 1 mm) to the largest microcrystal (1 to 0.5 mm) in the matrix, disregarding the cryptocrystalline and vitreous fractions.

Furthermore, chemical analyses of different mineral phases were performed for 45 of the samples, with an attempt to include the different lithological types and the entire spectrum of crystal sizes (from phenocrysts to microliths). Major elements, Ni, and Cr were analyzed in plagioclases (232 data), clinopyroxenes (199), amphiboles (128), orthopyroxenes (85), olivines (44), micas (12), and Fe–Ti oxides (124). Some zoned crystals and mineral inclusions were also included. The electron probe microanalyzer (EPMA–WDS brand JEOL model JXA–8900 M) at the Luis Bru Electronic Microscopy Center of the Universidad Complutense de Madrid (España) was used. Some points in the hyaline fraction of the matrix of some samples were randomly analyzed. For calculations of structural formulae and endmembers, the results whose total sum of percentages (%) of the elements analyzed, expressed as oxides, were lower than 95% (for silicates) or lower than 84% (for oxides) were discarded. To classify plagioclase, the relationship among Ab (NaAlSi₃O₈), Or

→
Figure 2. Geological map of the NHVC. Modified after Correa-Tamayo (2009). Notes: For the meaning of the acronyms of the volcano–stratigraphic units, see Table 4. Geological units of the basement: (Pznq) Quintero Gneiss, high-grade metamorphic quartzofeldspathic gneisses and quartzofeldspathic schists; (Pzmc) Cajamarca Complex, greenschists, quartz–micaceous schists, and quartzites; (J?bp) La Plata Batholith, diorite, quartz diorite, and granodiorite; (Kms) Cretaceous metasedimentary and sedimentary rocks, shales, phyllites, meta-sandstones, and fossiliferous limestones; (T?i) Tertiary intrusive rocks, andesitic and dacitic porphyries; (Q₂sd) Quaternary alluvial deposits, undifferentiated. Basement units are defined according to Hubach & Alvarado (1932), Orrego (1982), Orrego & París (1991), and Ingeominas (1995b).

Nevado del Huila Volcanic Complex



(KAlSi_3O_8), and An ($\text{CaAl}_2\text{Si}_2\text{O}_8$) was used. The compositional variation in olivine was examined as a function of changes in Fo. To classify the Fe–Ti oxides, the proportions of Usp and Mt (for magnetites and spinels), Usp, Mt, Chr, and Ple (for chromites), or Ilm and Hem (for ilmenites) were considered. For clinopyroxenes and orthopyroxenes, the classification method of Morimoto et al. (1988) was used according to variations among Wo ($\text{Ca}_2\text{Si}_2\text{O}_6$), En ($\text{Mg}_2\text{Si}_2\text{O}_6$), and Fs ($\text{Fe}_2\text{Si}_2\text{O}_6$). To classify the amphiboles, the nomenclature of Leake et al. (1997, 2004) for calcic amphiboles was used, and for micas, the PASP (phlogopite – annite / siderophyllite – polylithionite) classification system of Tischendorf et al. (2001) was used.

With mineral chemistry data, we sought to establish P–T conditions for magma crystallization through geothermometers and geobarometers based on equilibrium between two mineral phases (i.e., olivine–chromite and ilmenite–magnetite geothermometers), between the mineral and liquid phase (i.e., plagioclase–liquid, clinopyroxene–liquid, and olivine–liquid geothermobarometers), or in the composition of a mineral (i.e., the amphibole geothermometer and geobarometer). Furthermore, the oxidation state ($f\text{O}_2$) of the magma was measured based on the ilmenite–magnetite equilibrium relationship and the partition coefficient of FeO^* between plagioclase and liquid. For these calculations, several specific tools were used: the Cpx–Plag–Ol Thermobar program developed by Putirka (2005, 2008), the ILMAT program developed by Lepage (2003), and the PTMAFIC program developed by Soto & Soto (1995).

Nine isotopic dates were obtained using the whole–rock K–Ar method for representative samples of the NHVC (7) and its basement (2). Three of these dates were obtained from Geochron Laboratories (USA), and another six were obtained from Mass Spec Services (USA). Newly available isotopic dating using the $^{40}\text{Ar}/^{39}\text{Ar}$ method was achieved in the Argon Geochronology Laboratory of Oregon State University (USA), measured in groundmass of six other representative samples (Table 1).

To elucidate the main petrogenetic processes that formed the rocks that make up NHVC, to characterize the source area of the parent magma and to identify the mechanisms that led to its evolution from less differentiated magmas to more evolved ones, Sr and Nd isotope ratios were measured in five representative samples. These analyses were performed with the Micromass VG Sector 54 TIMS (thermal ionization mass spectrometer) at the Centro de Geocronología y Geoquímica Isotópica of the Universidad Complutense de Madrid.

3. Results

3.1. Geomorphological Characteristics

The morphology of the NHVC is the result of several sculpting agents: volcanic activity (mainly effusive) and erosion by glacial, fluvial, and gravitational processes (Figure 3).

The NHVC has an elongated ellipsoidal shape, 21.5 km in the N–S direction and 12 km in the E–W direction. Before the new dome was emplaced between 2008 and 2010 (Cardona et al., 2010; Pulgarín, 2012; Pulgarín et al., 2009), there were four peaks at its summit. The new summit is the fifth peak: the North Peak (5304 masl), La Cresta Peak (5284 masl), the Central Peak (5364 masl), the new dome (5297 masl, according to Cardona et al., 2010), and the South Peak (5052 masl), which has other associated smaller domes. In addition, the summit is covered by a glacier that in 1995 was 13.3 km² (Pulgarín et al., 1996, 2007). Prior to the eruptions in 2007, the glacier had been reduced to 10.4–10.5 km² (Cardona et al., 2010; Pulgarín et al., 2014). Recently, Instituto de Hidrología, Meteorología y Estudios Ambientales (2017) reported a glacial area of 7.5 km². For this chapter, an area of 8 km² was measured using an image from the Esri Map Viewer (Digital Globe) that was taken on 28 January 2016. The average height of the NHVC from the basement varies between 2300 and 2600 m. The approximate area at its base is 150 to 200 km², and the estimated volume of volcanic material is between 120 and 135 km³.

In addition, the NHVC has N–S and E–W symmetry, with steeper average gradients on the western (22° average) and eastern (21° average) slopes and lower gradients on the southern (14° average) and northern (13° average) slopes. The drainage pattern is radial, with a centrifugal arrangement with respect to the summit. The streams form confluences with a subparallel (N–S) principal drainage formed by the Páez River and its tributary, the Símbola River, which bound the volcano on the W and E sides, respectively.

The stepped relief of the NHVC was generated by the superposition of lava flows, which have escarpments that range from 5 to 300 m in height. According to the classification of denudation geofoms of volcanic origin from van Zuidam (1986), this relief corresponds to volcanic slopes in the categories V4 to V7, indicating steep to very steep, stepped volcanic slopes with moderate to very high inclination and moderate to severe degrees of dissection.

The categorization as a volcanic complex is based on several geomorphological characteristics, which were established following the various criteria defined in several classic references (Cas & Wright, 1987; de Silva & Francis, 1991; Francis, 1993; Short, 1986; van Zuidam, 1986): diverse individual volcanic geofoms, which overlap and have complex interrelationships; the absence of a single central cone; evidence of at least one sectoral collapse, in the form of a large dynamic slip; the peaks of the summit representing different emission centers; different degrees of dissection between the various overlapping superimposed lava layers; variations in the spatial distribution and direction of lava flows; and prominent geofoms, similar to *planèzes*, which represent remnants of a previous volcanic edifice.

Furthermore, mainly on the North Peak and Central Peak, several smaller volcanic geofoms are recognized: ogives or

Table 1. Isotopic data for representative samples of the NHVC (13) and its basement (2).

Sample	Geological unit	Type of sample	Method	Technical specifications	Age
ACNH428	Q ₁ an	Rock in situ, porphyritic andesite	⁴⁰ Ar/ ³⁹ Ar	Incremental heating. In groundmass. Plateau age. Eruption age.	29.8 ± 12.6 ka
ACNH401	Q ₁ pn	Rock in situ, porphyritic andesite	⁴⁰ Ar/ ³⁹ Ar	Incremental heating. In groundmass. Plateau age. Eruption age.	109.2 ± 4.4 ka
BPNH341	Q ₁ ps	Rock in situ, porphyritic andesite	K/Ar	Bulk rock*. ⁴⁰ Ar** 0.001(0). % ⁴⁰ Ar 11.9–10.1. %K 1.95.	0.13 ± 0.02 Ma
ACNH403	Q ₁ pc	Rock in situ, porphyritic andesite	K/Ar	Bulk rock*. ⁴⁰ Ar** <0.001. % ⁴⁰ Ar <1. %K 1.58.	<0.2 Ma
BPAV97	Q ₁ ps?	Rock in situ, lava layer sample below Q ₁ ae	K/Ar	Bulk rock*. ⁴⁰ Ar** <0.001. % ⁴⁰ Ar <1. %K 1.29.	<0.2 Ma
BPNH337	Q ₁ ps	Rock in situ, porphyritic andesite	⁴⁰ Ar/ ³⁹ Ar	Incremental heating. In groundmass. Total fusion only. Age a minimum estimate.	272.2 ± 21.7 ka
ACNH413	Q ₁ ls	Rock in situ, porphyritic andesite	⁴⁰ Ar/ ³⁹ Ar	Incremental heating. In groundmass. Plateau age. Eruption age.	285.6 ± 5.3 ka
ACNH412	Q ₁ lm	Rock in situ, porphyritic andesite	⁴⁰ Ar/ ³⁹ Ar	Incremental heating. In groundmass. Plateau age. Eruption age.	291.9 ± 5.1 ka
BPNH307	Q ₁ li	Rock in situ, porphyritic andesite	⁴⁰ Ar/ ³⁹ Ar	Incremental heating. In groundmass. Plateau age. Eruption age.	306.6 ± 7.2 ka
VNH3a	Q ₁ li?	Fragment of porphyritic rock, near laguna de Páez	K/Ar	Bulk rock*. ⁴⁰ Ar** 0.001(9)–0.001(5). % ⁴⁰ Ar 5.8–5.6. %K 1.45.	0.3 ± 0.2 Ma
VNH33	Q ₁ pn	Rock in situ, porphyritic andesite	K/Ar	Bulk rock*. ⁴⁰ Ar** 0.003(2)–0.002(9). % ⁴⁰ Ar 15.9–10.4. %K 1.92.	0.4 ± 0.1 Ma
VNH56a	Q ₁ ps?	Lava layer sample within Q ₁ ae	K/Ar	Bulk rock*. ⁴⁰ Ar** 0.005(1)–0.004(9). % ⁴⁰ Ar 12.2–15.3. %K 1.58–1.57.	0.8 ± 0.2 Ma
BPAV90A	Q ₁ ps?	Fragment of porphyritic rock in Q ₁ ae	K/Ar	Bulk rock***. ⁴⁰ Ar** 0.000194–0.000138. % ⁴⁰ Ar 3.30–4.10. %K 1.563–1.553.	1.5 ± 0.1 Ma
BPAV90	Kd	Rock in situ, mafic, porphyritic dike that cuts J?bp	K/Ar	Bulk rock***. ⁴⁰ Ar** 0.005731–0.005691. % ⁴⁰ Ar 38.10–36.40. %K 0.802–0.916.	93.5 ± 2.6 Ma
BPAV100	J?bp	Rock in situ, granodiorite	K/Ar	Bulk rock***. ⁴⁰ Ar** 0.01280–0.01257. % ⁴⁰ Ar 51.3–48.3. %K 1.392–1.426.	125 ± 3 Ma

Note: ⁴⁰Ar/³⁹Ar data by the Argon Geochronology Laboratory of the Oregon State University (USA) in 2016.

*Data provided by the Teledyne (USA) or Mass Spec Services (Old Teledyne).

**⁴⁰Ar radiogenic expressed as ppm by Geochron Laboratories (USA) or as scc/gm × 10⁻⁵ by Teledyne.

***Data commissioned to Geochron Laboratories (USA) by Doctor José Luis MACIAS (professor of the Universidad Nacional Autónoma de México).

lava with wave-like ridges, blocky lava or short block flows, and structures in the form of levees or lateral ridges. There are also volcanic domes, among which Morro Negro and El Cerrillo stand out to the south of the summit of the South Peak, and the new dome is located between the Central Peak and South Peak.

The lava flows descended to minimum elevations of 2000 masl (towards the S), 2600 masl (towards the E and W), and 3200 masl (towards the N). The maximum distances traveled correspond to lava flows in the lower part of the main edifice: 3 to 4 km (N) and 10 to 12 km (S), with an average between 9 and

10 km. The shorter flows (1 to 2.5 km) ensued from the North Peak. The best-preserved lava flow stacks are above 4300 masl on the North Peak and Central Peak. The high degree of hydrothermal alteration, the marked dissection, and the intense glacial sculpting of the rocks in the upper part of the South Peak suggest that these rocks are older than equivalent rocks in the North Peak and Central Peak.

The most remarkable glacial geoforms are glacial cirques, U-shaped valleys, glacial lakes, and hanging valleys. The lateral moraines were very useful because their wide elevation distribution allows them to be separated into different groups

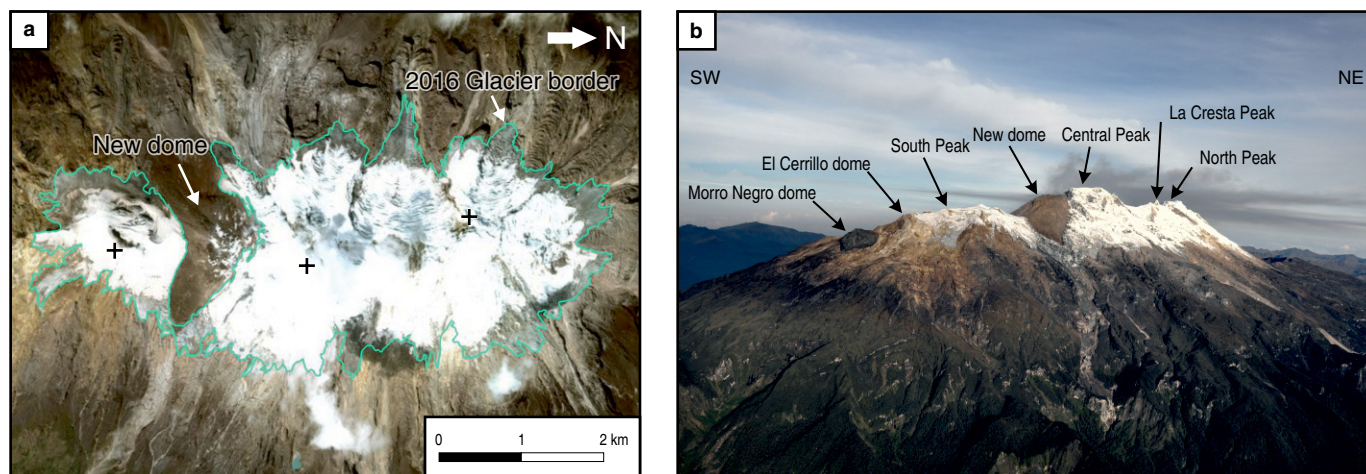


Figure 3. Satellite and aerial panoramas of the NHVC. **(a)** Nevado del Huila area. Digital Globe image, 0.50 m resolution (Base Map Services of Esri), 28 January 2016. The new dome can be seen in relation to the boundaries of the glacier (green solid line). **(b)** NHVC seen from the southeast; the Morro Negro dome and the North Peak are separated by approximately 5 to 6 km. Photograph by Servicio Geológico Colombiano through helicopter overflight on 25 January 2011.

defining eight glacial stages, named consecutively from Huila1 (the oldest) to Huila8 (the most recent; Table 2).

The correlation between these eight glacial stages and those recognized in other glacial zones of Colombia (mainly in the Parque Nacional Natural Los Nevados) allows us to conclude that the NHVC glacial stages occurred successively, perhaps from the Penultimate Glaciation, the Last Interglacial, or the Last Glaciation, from more than 100 000 years ago until recently, including the Pleniglacial and the Little Ice Age, which are recorded for this area of the Central Cordillera between 4000 and 4250 masl (Flórez, 1992; Herd, 1982). In addition, after the Pleniglacial, four glacial stages occurred from the Huila5 stage to the Huila8 stage. The Huila2 to Huila6 glacial stages coincide with the wide area of glacial deposits and geomorphs that formed during the Last Glaciation and also include glaciofluvial deposits. This area is located in the periglacial zone of the NHVC, below 4000 ± 200 masl. It is nearly continuous, descends to 3600 masl, encircles almost the entire edifice and has served as a marker to separate the most recent units in the higher part from the other lower units. This belt belongs to the morphological glacial zone inherited with a volcanic influence (between 3800 ± 100 m and 3000 ± 200 m), which in the Colombian territory represents an area that was occupied by glaciers during the Last Glaciation, from 35 000 to 10 000 years ago (Instituto de Hidrología, Meteorología y Estudios Ambientales, 1996).

In Colombia, it has been established that mountain glaciers such as the Nevado del Huila are vestiges of the Last Glaciation (Flórez, 1992; Flórez & Ochoa, 1990), which began 115 000 years ago, with maximum ice extent (Pleniglacial) between 45 000 and 25 000 years ago (van der Hammen, 1981). The climatic change that caused the growth of these glaciers corresponds to the Little Ice Age or Neoglacial Age, between 1600 and 1850 AD (Herd, 1982; Flórez, 1992).

Based on the geomorphological analysis of the NHVC, three main sets of lava layers were distinguished, each with distinctive morphological characteristics. Based on these morphological differences, two volcanic edifices were identified: the Pre-Huila edifice (Pre-Huila) and the Huila edifice (Huila), along with three stages of eruptive history including the Pre-Huila Stage (PHS), Ancient Huila Stage (AHS), and Recent Huila Stage (RHS).

The remnants of the oldest volcanic edifice, Pre-Huila, which perhaps was 4000 to 4200 masl and was built during the PHS, currently correspond to the lower part of the slopes, with more “evolved” morphology, a greater degree of dissection and steeper relief, in which the original volcanic geomorphs have been erased due to surface erosion, glacial action, hydrothermal alteration, weathering, active faults, and mass wasting processes. The middle section of these slopes corresponds to the remains of part of the Huila edifice that was built during the AHS, which perhaps reached 4600 to 4700 masl. These remnants show less modified morphology with less-dissected and lower-gradient relief and well-preserved volcanic geomorphs in the northern and central sections. The highest part, up to its current maximum elevation (5364 masl), represents the RHS, where the original volcanic geomorphs are better preserved and are easily recognized.

According to Pulgarín (2000), the Upper Pleistocene Páez Debris Avalanche was generated by gravitational collapse, was not of magmatic origin, and occurred on the southern flank of the NHVC. At some time between 200 000 and 46 000 years ago, this event affected Pre-Huila and rocks from the AHS. The avalanche would have dammed the Páez River, which, upon rupturing, generated a large debris flow whose deposits are presently identified as terraces with maximum heights of 150 m along the river banks.

Table 2. Glacial stages in the NHVC correlated with glacial stages defined in PNNN*.

Glacial stages–NHVC (masl)	Glacial stages–PNNN (masl)	Age according to correlation**
Huila8 (4300–4550)	Late Ruiz (4200–4600)	<AD 1800
Huila7 (4000–4250)	Early Ruiz–late Santa Isabel (4150)	AD 1600–1800
Huila6 (3700–3950)	Late Otún (3800–4000)	10 000–11 000 years BP
Huila5 (3500–3650)	Late Murillo (3500–3600)	14 000–20 000 years BP
Huila4 (3200–3450)	Early Murillo (3400–3500)	25 000–28 000 years BP
Huila3 (3050–3100)	Late Río Recio (3300)	34 000–40 000 years BP
Huila2 (2850–3000)	Early Río Recio (2900–3300)	>48 000 years BP
Huila1 (2650–2800)	–	>100 000? years BP

Note: (PNNN) Parque Nacional Natural Los Nevados.

*Modified after Pulgarín & Correa–Tamayo (2003).

**Defined age based on correlation made by Pulgarín & Correa–Tamayo (2003).

The separation between the AHS and RHS was defined by morphological differences and the existence of a wide belt of deposits and glacial geoforms below 4000 ± 200 masl that formed during the Last Glaciation, which ended near the Pleistocene – Holocene boundary after intense glacial erosion sculpted the upper rocks of the AHS, forming large glacial valleys that were later invaded by new RHS lava flows during the Holocene.

To explain the presence of the cuchilla de Verdún, which is a towering sharp peak located to the north of the main structure of the NHVC and separated from it by a deep, half–moon–shaped valley, there are three possible alternatives: (1) formation of a collapse structure, which took advantage of a zone of previous weakness because it is located at the intersection of faults; (2) remains of the edge of a small caldera (diameter <4 to 5 km) that is a trapdoor or piston collapse (Cole et al., 2005) caused by subsidence or simple collapse in an effusive regime and not necessarily associated with a large explosive event; and (3) ancient gravitational slope collapse in the northern region, which perhaps occurred towards the end of the PHS or beginning of the AHS, similar to the gravitational collapse in the southern flank in the Late Pleistocene.

By comparing the elevation ranges for the three stages in the eruptive history of the NHVC with the elevations and ages of its eight glacial stages (Table 3), there was a first approximation of the age ranges that comprise the volcanic stages, given that if the moraines of glacial stage Huila6 (between 10 000 and 11000 years ago) did not affect the rocks of the RHS, this should have started 10 000 to 11 000 years ago at the beginning of the Holocene. Additionally, the AHS units would have an age greater than 10 000–11 000 years old. Furthermore, the age of the moraines of the glacial stage Huila1 allows the inference that the age of the rocks of the PHS is greater than 100 000 years; thus, the AHS lasted from 100 000 to 10 000 years ago. The

glacial stages Huila7 and Huila8, which were produced during the Neoglacial Age (1600 to 1800 AD), affected the RHS rocks.

3.2. General Volcanic Stratigraphy

To characterize the stages of eruptive history of the NHVC, stratigraphic criteria and macroscopic analyses were considered: the distribution of the lava flow stacks with respect to possible eruptive centers; elevational position, when it was a clear indicator of the superposition relationships between the lava layers; structural and textural changes; variations in the degree of weathering; the presence of possible contact surfaces; and compositional differences.

In the NHVC, there are predominantly superimposed lava layers in thick stacks that appear in walls up to 200 m high. In general, some of these layers show a structure that is a typical “sandwich” with a massive central body (10 to 50 m thick) between layers of associated autobrecciated lavas at the base and/or top (≤ 5 to 10 m). Columnar and pseudocolumnar jointing are common, and subhorizontal jointing is also common. The degree of weathering is moderate to high and is lower in rocks of the RHS in the Central Peak and North Peak. Rocks from the RHS with the highest degree of hydrothermal alteration are in the South Peak.

In general, the texture in hand samples is porphyritic with medium to fine crystal sizes. In some cases, it is almost aphanitic. On a fresh surface, the color varies from dark to very light gray, sometimes very dark gray to almost black. Additionally, flow banding and flow texture are common. In some cases, the banding is reddish, perhaps caused by syneruptive oxidation. Some rocks from the RHS in the Central Peak and North Peak are slightly more equigranular and are lighter in color.

The content of phenocrysts is very low (1 to 2%, rarely up to 5%), and the phenocrysts are mainly plagioclase with a few

Table 3. Comparison between the volcanic stages in the eruptive history of the NHVC and its glacial stages*.

Stages of eruptive history NHVC (masl)	Glacial stages NHVC (masl)	Age glacial stage according to correlation** with glacial stages of PNNN
Recent Huila (>4300 ± 100)	Huila8 (4300–4550)	<AD 1800
	Huila7 (4000–4250)	AD 1600–1800
	Huila6 (3700–3950)	10 000–11 000 years BP
	Huila5 (3500–3650)	14 000–20 000 years BP
Ancient Huila (4300 ± 100 to 3600 ± 200)	Huila4 (3200–3450)	25 000–28 000 years BP
	Huila3 (3050–3100)	34 000–40 000 years BP
	Huila2 (2850–3000)	>48 000 years BP
Pre-Huila (3600 ± 200 to 2600 ± 100)	Huila1 (2650–2800)	>100 000? years BP

Note: (PNNN) Parque Nacional Natural Los Nevados.

*Modified after Correa-Tamayo (2009).

**Defined age based on correlation made by Pulgarín & Correa-Tamayo (2003).

mafic minerals (amphiboles). The fraction of smaller crystals includes feldspars and mafic minerals (pyroxenes ± amphibole). The matrix is aphanitic. In addition, there are small, fine aggregates of mafic minerals. It is common to find rounded to subrounded enclaves of finer to aphanitic texture and darker or reddish color (autoliths?). There are also enclaves of rocks with medium to fine granitic textures (xenoliths).

The clearest evidence of explosive activity corresponds to three layers of concentrated pyroclastic density currents, consisting of blocks and ashes, and a fourth layer of ashes and pumice, located in the upper part of the eastern flank of the Central Peak. The most recent features are the domes that have been extruded in the upper part between the Central Peak and South Peak.

The synthesized stratigraphy is shown in the corresponding geological map (see Figure 2) and in four generalized columns (Figure 4), three of which correspond to the three main peaks representing three different eruption centers. In these columns, the three stages of eruptive history are represented. The fourth column corresponds to the northernmost lava layers in the area of the laguna de Páez. Thirteen volcano-stratigraphic units are defined, each corresponding to a set of lava flow layers that, due to their morphological and lithological characteristics and location, are recognized as a homogeneous group representing a specific time interval in the eruptive history of the NHVC.

The nomenclature (Table 4) used to designate these units is based on the following criteria: (1) relative age established by correlation; (2) stage of eruptive history; (3) geographic location, including the relative stratigraphic position for the sector of the laguna de Páez (i: lower, m: middle, and s: upper); and (4) type of deposit or its origin. The total thickness of each unit is determined according to maximum and minimum heights of outcrops, represented on the geological map.

The isotopic dates support the eruptive history, revealing a more precise chronological framework. According to dating, either by K–Ar or $^{40}\text{Ar}/^{39}\text{Ar}$ of representative Pre-Huila samples, its age is early Pleistocene (Calabrian, 1.5 Ma) to Middle Pleistocene (between 0.13 and 0.8 Ma). Huila is younger, with Late Pleistocene to Holocene ages (Figure 5). Regarding the duration of each stage, it is clear that the longest stage corresponds to the PHS, which is in accordance with the wide spatial distribution and the total thickness of its units, mainly in the southern sector. Meanwhile, the AHS and RHS, which are younger, are shorter.

In short, the eruptive history of the NHVC began at 1.5 Ma, in the early Pleistocene (Calabrian), with the PHS. Later, 100 000 years ago, the AHS began and lasted for a shorter duration between 80 000 and 90 000 years in the Late Pleistocene. At some time between the end of the PHS and the beginning of the AHS, the construction of the NHVC was strongly interrupted by a large destructive event through the nonmagmatic south flank collapse (ca. 200 000 to 46 000 years ago, according to Pulgarín, 2000; Pulgarín et al., 2004), which emplaced a sequence of debris avalanche and debris flow deposits that modified the topographic and hydrographic conditions of this area. When the Last Glaciation ended, which perhaps was accompanied by a decrease in eruptive activity, the RHS should have started during the Holocene.

3.3. Petrographic Characteristics

The representative rocks of the NHVC are mesocratic to leucocratic with textures that vary among microporphyritic, seriate microporphyritic, and microcrystalline (Figure 6). The content of phenocrysts is low ($\leq 2\text{--}6\%$), whereas the fraction of microphenocrysts is greater ($\leq 3\text{--}28\%$). The percentage of matrix is predominant ($\geq 83\text{--}94\%$) and varies from microcrystalline to

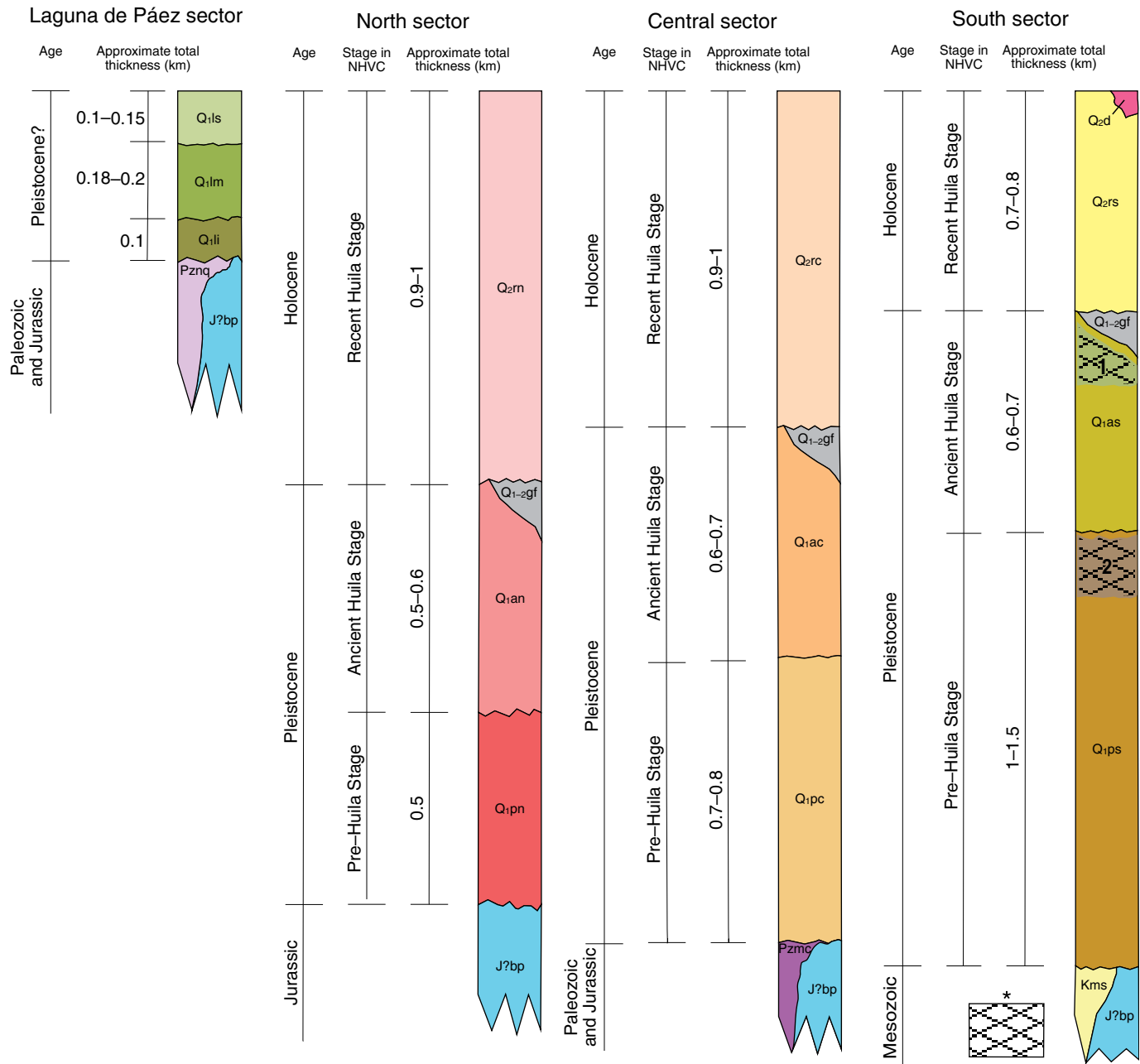


Figure 4. Generalized stratigraphic columns in which the 13 volcano–stratigraphic units of the NHVC are represented. Modified after Correa–Tamayo & Ancochea (2015a). Notes: for the meaning of the acronyms of the volcano–stratigraphic units, see Table 4. *The hatched symbols in 1 and 2 indicate the relative moment in which the Páez Debris Avalanche (Q₁ae) could have occurred: (1) according to Pulgarín (2000); (2) according to Correa–Tamayo (2009).

cryptocrystalline and can be holocrystalline, hypocrySTALLINE or hypohyaline, and rarely holohyaline (Figure 7).

Microcrystalline polymineral aggregates (pyroxenes ± olivine ± opaque minerals, pyroxenes ± plagioclases ± opaques minerals) and monomineral aggregates or glomerocrysts are abundant, some of which may have formed in the early stages of crystallization. They are frequent microenclaves in volcanic rock (autoliths?), and some may be the result of magmatic mingling. Occasionally, there are microenclaves of granitic rock

(xenoliths). Microcrystalline aggregates of amphiboles are frequent in Q₂d, Q₂rc, and Q₂rn.

Indicators of some degree of devitrification are the presence of spherulites, incipient perlitic texture, and/or small cryptocrystalline portions in a partially vitreous matrix. In almost all samples, there is textural evidence of disequilibrium processes: resorption rims, rounded and/or engulfed borders, reaction rims, opaque borders in amphiboles, skeletal forms, partial or total pseudomorphism of oxides in amphiboles, and sieve textures

Table 4. List of stratigraphic units defined in the NHVC.

Acronym	Relative age	Volcanic stage	Geographic location	Type of deposits	Volcano–stratigraphic unit		
Q ₂ d	Holocene (Q ₂)	Recent Huila Stage (r)	South and center	Domes (d)	Domes of the Recent Huila Stage		
Q ₂ rn			Northern sector (n)		Lavas of the Recent Huila Stage in the North Peak		
Q ₂ rc			Central sector (c)	Lava flows	Lavas of the Recent Huila Stage in the Central Peak		
Q ₂ rs			Southern sector (s)		Lavas of the Recent Huila Stage in the South Peak		
Q ₁₋₂ gf	Pleistocene – Holocene (Q ₁₋₂)	AHS ↔ RHS	Scattered	Glacial and fluvio-glacial deposits (gf)			
Q ₁ an	Pleistocene (Q ₁)	Ancient Huila Stage (a)	Northern sector (n)		Lavas of the Ancient Huila Stage in the north sector		
Q ₁ ac			Central sector (c)	Lava flows	Lavas of the Ancient Huila Stage in the central sector		
Q ₁ as			Southern sector (s)		Lavas of the Ancient Huila Stage in the south sector		
Q ₁ ae			PHS ↔ AHS	To the south	Debris avalanche (ae)		
Q ₁ ls			≈ PHS			Lavas of the upper unit of the laguna de Páez sector	
Q ₁ lm				Laguna de Páez sector (l)*	Lava flows	Lavas of the intermediate unit of the laguna de Páez sector	
Q ₁ li						Lavas of the lower unit of the laguna de Páez sector	
Q ₁ pn			Pre–Huila Stage (p)		Northern sector (n)		Lavas of the Pre–Huila Stage in the north sector
Q ₁ pc					Central sector (c)	Lava flows	Lavas of the Pre–Huila Stage in the central sector
Q ₁ ps					Southern sector (s)		Lavas of the Pre–Huila Stage in the south sector

Note: (PHS) Pre–Huila Stage; (AHS) Ancient Huila Stage; (RHS) Recent Huila Stage.

*Units of the laguna de Páez sector separated into three groups according to relative stratigraphic position (i: inferior = lower, m: media = middle, and s: superior = upper).

(in plagioclase). The flow texture and flow banding are most noticeable in hand specimens. Glass also appears as inclusions in plagioclase, in microvesicle walls or interstitially in microcrystalline aggregates.

The three main mineral phases are (Figures 8, 9) plagioclase (10–58 %), clinopyroxene ($\leq 11\%$), and amphibole ($\leq 14\%$, maximum 19% in Q₂d). Orthopyroxene ($\leq 6\%$) is an accessory phase. Other accessory minerals include micas ($\leq 5\%$), olivine ($\leq 4\%$), and apatite. Plagioclase appears as phenocrysts, microphenocrysts, microcrystals, and microlites; clinopyroxenes and amphiboles occur as microphenocrysts or microcrystals and sometimes as phenocrysts; orthopyroxenes, micas, and olivines occur as microcrystals. Opaque microcrystals ($\leq 14\%$), which correspond to Fe–Ti oxides, are in the matrix of most samples. In addition to glass inclusions, mainly in plagioclases (sieve texture), it is also common to find inclusions of opaque minerals and pyroxenes inside other pyroxenes and amphiboles.

The strong pleochroism of the amphiboles is highly variable. In some crystals, it varies between light greenish brown and dark brown, which is typical of hornblende. Others show

pleochroism that changes from light reddish brown to very dark reddish brown, typical of the so-called oxyhornblende. Due to their optical characteristics, micas are classified within the biotite–phlogopite group.

The Q₁ps, Q₁as, Q₂rs, Q₁li, and Q₁lm units have higher contents of anhydrous minerals (clinopyroxene \pm orthopyroxene) than hydrated minerals (amphibole \pm biotite). Meanwhile, Q₂d, Q₂rc, Q₂rn, and Q₁ls have higher percentages of hydrated minerals (i.e., amphibole) than anhydrous minerals (i.e., orthopyroxene). The Q₁ac unit and some samples of Q₁an and Q₂rn represent an intermediate situation (Figure 10).

Based on detailed compositional variations, several petrographic types are identified. In Q₁ps, Q₁pc, and Q₁pn are two-pyroxene andesites (clinopyroxene + orthopyroxene), and the clinopyroxene andesites predominate, with or without orthopyroxene. The rocks of Q₁as, Q₁ac, and Q₁an are mainly clinopyroxene andesites, amphibole–clinopyroxene andesites, and clinopyroxene–amphibole andesites.

Although the rocks of Q₂rs are characterized by an advanced state of hydrothermal alteration, some fresh samples

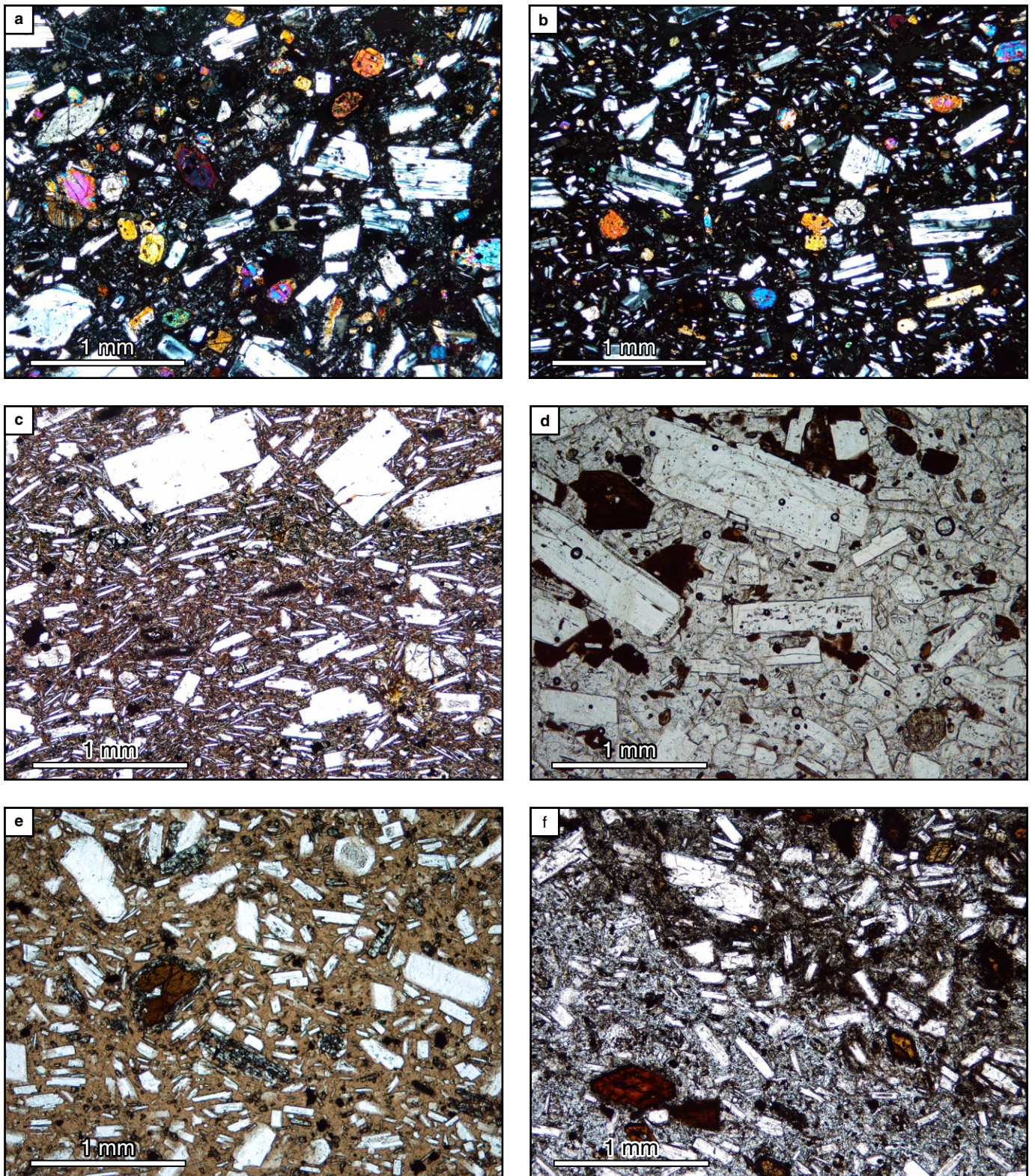


Figure 6. Main textural characteristics of NHVC lavas. **(a, b)** Very fine seriate microporphyritic to microcrystalline textures in clinopyroxene andesite with orthopyroxene (sample ACNH411 from Q_{1li}). **(c)** Clinopyroxene andesite with flow texture (sample BPNH135 from Q_{2rs}). **(d)** Amphibole-clinopyroxene andesite with partially vitreous matrix and incipient perlitic texture (sample BPNH328 from Q_{3ac}). **(e)** Amphibole-clinopyroxene andesite, with high glass content in the matrix (sample ACNH407 from Q_{1li}). **(f)** Amphibole-clinopyroxene andesite, with flow texture and banding texture (sample ACNH414 from Q_{1li}).

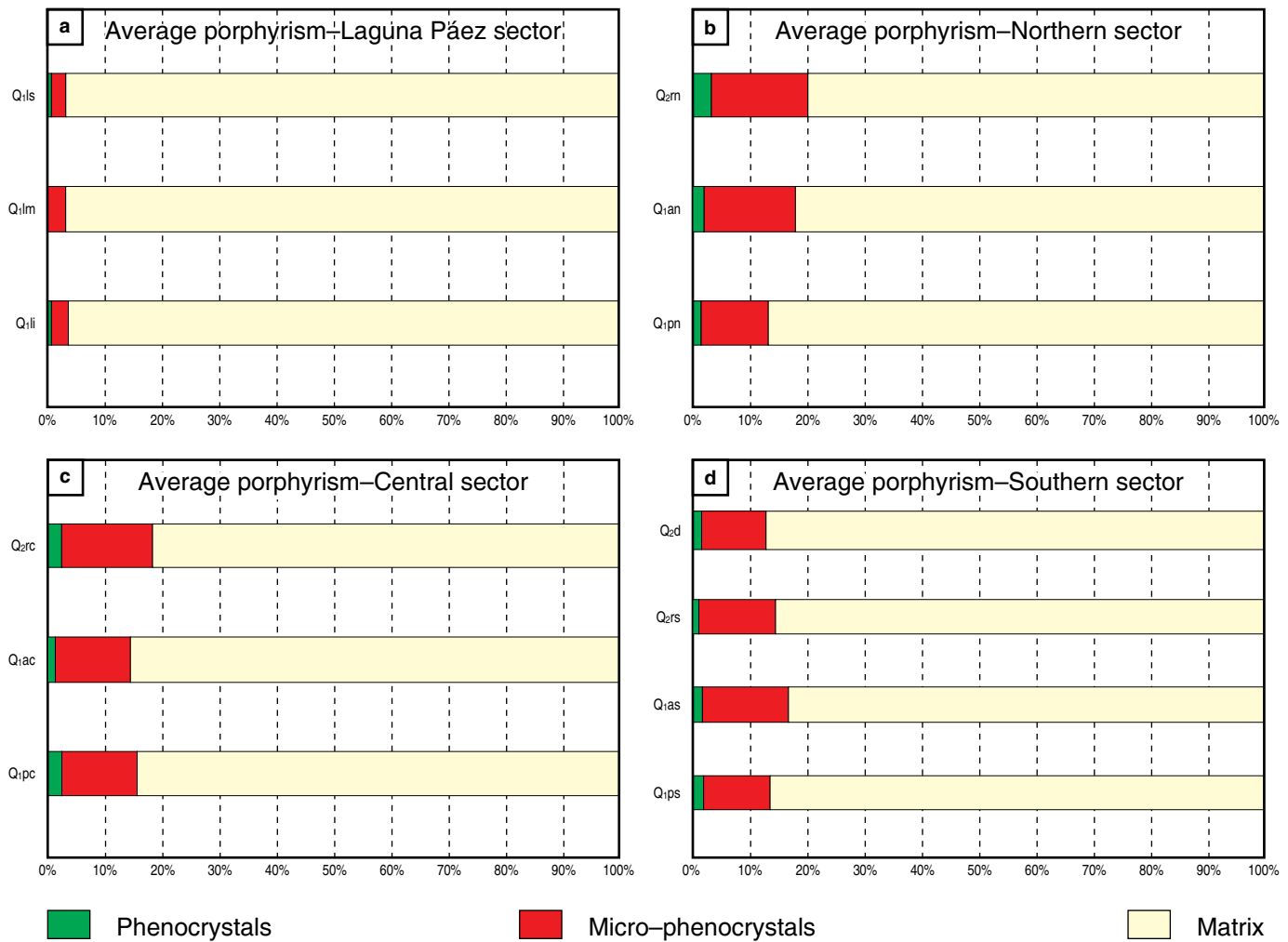


Figure 7. Variations in the average value of “porphyryism” in each of the 13 volcano–stratigraphic units of the NHVC. Modified after Correa–Tamayo (2009).

are identified as clinopyroxene andesites. The Q₂rc and Q₂rn units consist of amphibole andesites, amphibole–clinopyroxene andesites, and clinopyroxene andesites, whereas Q₂d contains primarily amphibole andesites and amphibole–clinopyroxene andesites. The most characteristic petrographic feature in more recent rocks of the NHVC is the relative increase in amphibole content, especially in Q₂rc and Q₂rn, and likewise in Q₂d.

The Q₁li and Q₁lm units essentially have andesites with two pyroxenes and clinopyroxene, whereas Q₁ls are amphibole–clinopyroxene andesites. Thus, these three units are intermediate between the PHS and AHS.

3.4. Mineral Chemistry

The composition of plagioclase varies between labradorite (An₆₀) and oligoclase (An₂₃), with predominantly andesine and a proportion of orthoclase less than Or₁₀ (Figure 11). Furthermore, these grains show normal, reverse, and oscillatory zoning.

The clinopyroxenes are mainly augites and secondarily, diopside (Figure 12a), with a wide compositional range (En_{54–24}, Wo_{49–35}, and Fs_{16–1}). Reverse zoning, with borders richer in magnesium (contents En₅₂) than centers (contents En₄₃), and normal zoning, with borders that are less rich in magnesium (En₄₂) than centers (En₄₉), are present.

The compositional range of orthopyroxenes is relatively narrow (En_{76–67}, Wo_{≤3}, and Fs_{≤33}), all in the enstatite field (Figure 12b) of the classification diagram from Morimoto et al. (1988). In microcrystals with slight reverse zoning, the Mg content tends to increase from the core to the border.

In the classification diagram for calcium amphiboles from Leake et al. (1997), most are represented in the field of the magnesium–hastingsite series, and only a few fall within the field of edenites (Figure 13a). Magnesiohornblende and tschermakite are scarce (Figure 13b). These grains have normal and reverse zoning in almost equal proportions. Oscillatory zoning is the scarcest. From the center to the edge of the crystals, the

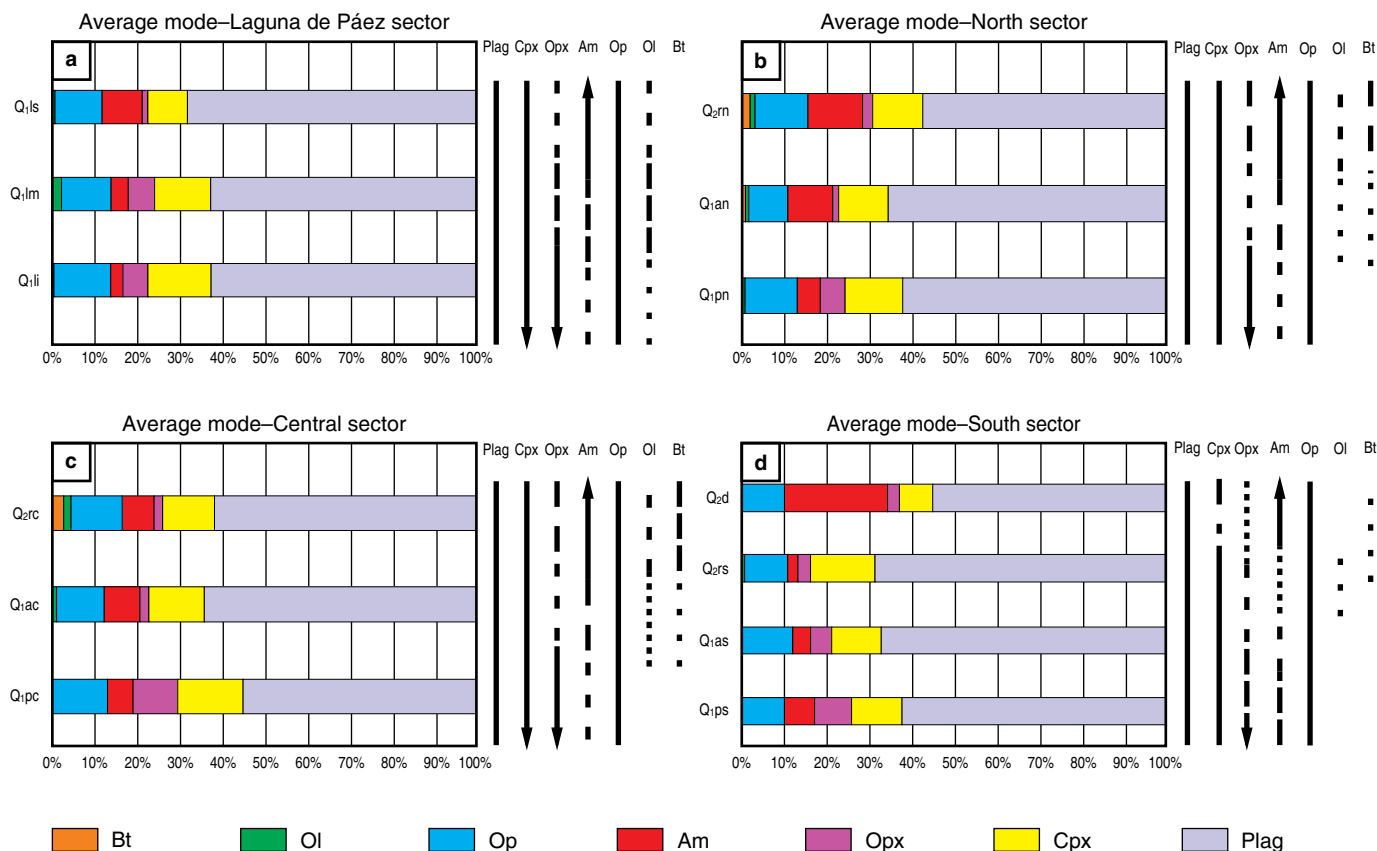


Figure 8. Variations in the average values of the modal contents of the main mineral phases in each of the 13 volcano-stratigraphic units of the NHVC. Modified after Correa-Tamayo (2009). The vertical lines indicate the relative variations in the modal contents (dotted line indicates accessory or sporadic presence), and the arrow indicates where it decreases or increases.

composition changes from edenite to magnesium-hastingsite, and vice versa.

Among the Fe-Ti oxides (Figure 14), there are predominantly magnetites (Usp_{36-2}) and ulvite (Usp_{100-64}); both sometimes appear in intimate association as exsolution lamellae. There are some chromites (Usp_{3-1} , Mt_{19-13} , Ple_{33-28} , and Chr_{56-49}) as inclusions in olivine and a few ilmenites (Hem_{36-25}).

The range of composition of the olivines varies from Fo_{91} to Fo_{79} . Some show slight compositional zoning, typical in this type of rock, from centers that are rich in Mg (Fo_{88-85}) to borders that are less rich in Mg (Fo_{86-79}). Because of textural characteristics (i.e., borders of corrosion and/or resorption, reaction rims, skeletal forms, and glomeroporphyritic aggregates) and compositional characteristics, some olivines could be xenocrysts in partial disequilibrium with the matrix that surrounds them.

The micas have very homogeneous compositions. They are phlogopites with a very narrow variation range (Phl_{75-71} and Ann_{30-25}) and a high Mg content. In the PASP (phlogopite – annite / siderophyllite – polyolithionite) classification system from Tischendorf et al. (2001), the micas remain in the field of biotites that are rich in Mg, near the field of phlogopites,

following the line of variation between ferro-phlogopite and phlogopite (Figure 15).

The composition of the vitreous fraction of the matrix is rhyolitic ($SiO_2 > 71\%$), and the composition of some components in the cryptocrystalline fraction is equivalent to feldspar that varies between andesine-oligoclase plagioclase and anorthoclase or sanidine potassium feldspar.

3.5. Estimation of the Conditions (fO_2 and P-T) of Crystallization

The oxidation state of the magma (fO_2) and the P-T conditions of crystallization were calculated using different geothermometers and geobarometers based on the chemical composition of the main mineral phases of the NHVC and the corresponding melts.

From data obtained in two ilmenite-magnetite pairs that were analyzed in sample ACNH411 and using the program ILMAT, temperature values were obtained between 884 and 808 °C; oxygen fugacity ranged (fO_2) between $10^{-10.6}$ and $10^{-12.6}$ corresponding to 1.7 and 1.0 log units between the HM (hematite-magnetite) and QFM (quartz-fayalite-magnetite) curves,

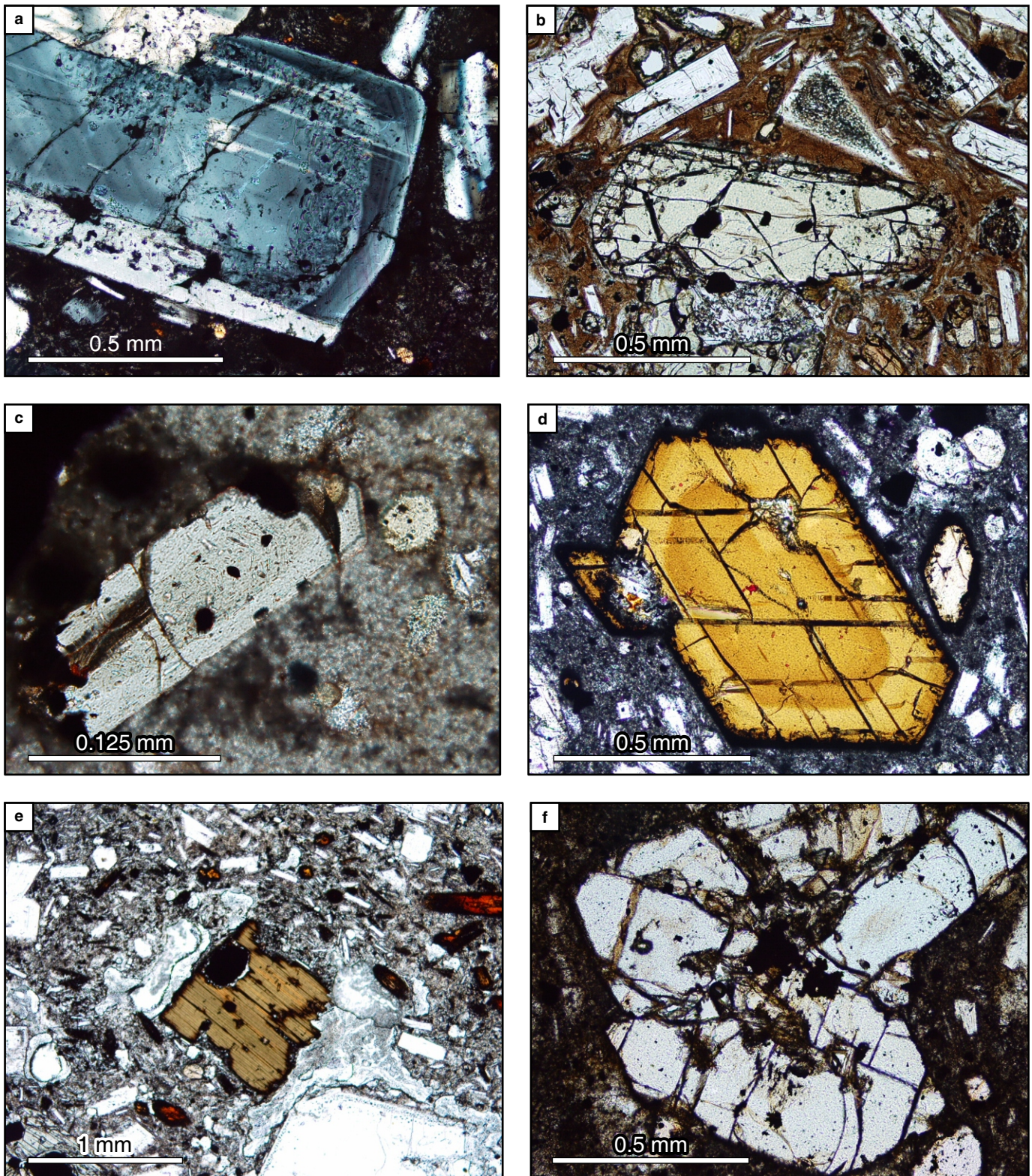


Figure 9. Main mineral phases of the NHVC rocks: **(a)** Plagioclase, **(b)** Clinopyroxene, **(c)** Orthopyroxene, and **(d)** Amphibole. Main accessory minerals: **(e)** Micas and **(f)** Olivine.

which indicates oxidizing conditions in the magma (Figure 16). Higher temperature values (903 to 861 °C) were obtained with the geothermometer of Powell & Powell (1977).

By applying the olivine–chromite geothermometer of Fabriès (1979) and using the program PTMAFIC, from chromite inclusions ($\text{Cr}^* 58\text{--}51 > \text{Al}^* 34\text{--}29 > \text{Fe}^* 18\text{--}12$) in olivine

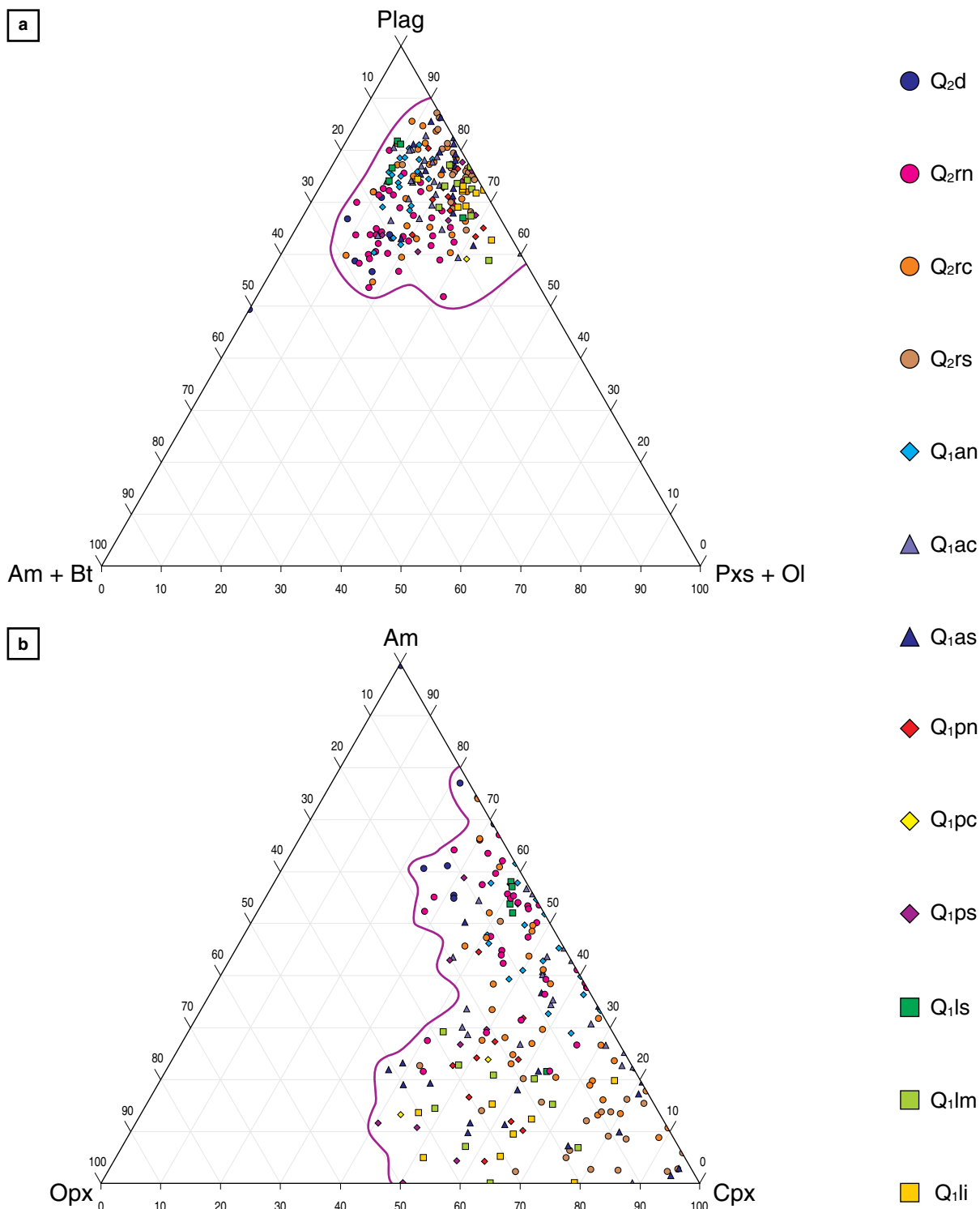


Figure 10. Ternary diagrams for detailed petrographic classification of andesitic samples that are representative of the 13 volcano-stratigraphic units of the NHVC, according to the percentages of the main mineral phases, identified as phenocrysts, microphenocrysts, or in the matrix. **(a)** Plagioclase (Plag), Pyroxenes (Pxs) + Olivine (Ol), Amphibole (Am) + Biotite (Bt). **(b)** Amphibole (Am), Clinopyroxene (Cpx), Orthopyroxene (Opx). Modified after Correa-Tamayo (2009).

(Fe_{89-85}) from some samples of Q_{2rc} and Q_{2rn} , a temperature range between 1085 and 1059 °C was established for the primary crystallization of the olivine–chromite pair. A second temperature interval is between 884 and 864 °C.

Using the calculation program Cpx–Plag–Ol Thermobar, several olivine–liquid and clinopyroxene–liquid geothermometers and several clinopyroxene–liquid and plagioclase–liquid geothermobarometers were calculated. Specifically, the crystal-

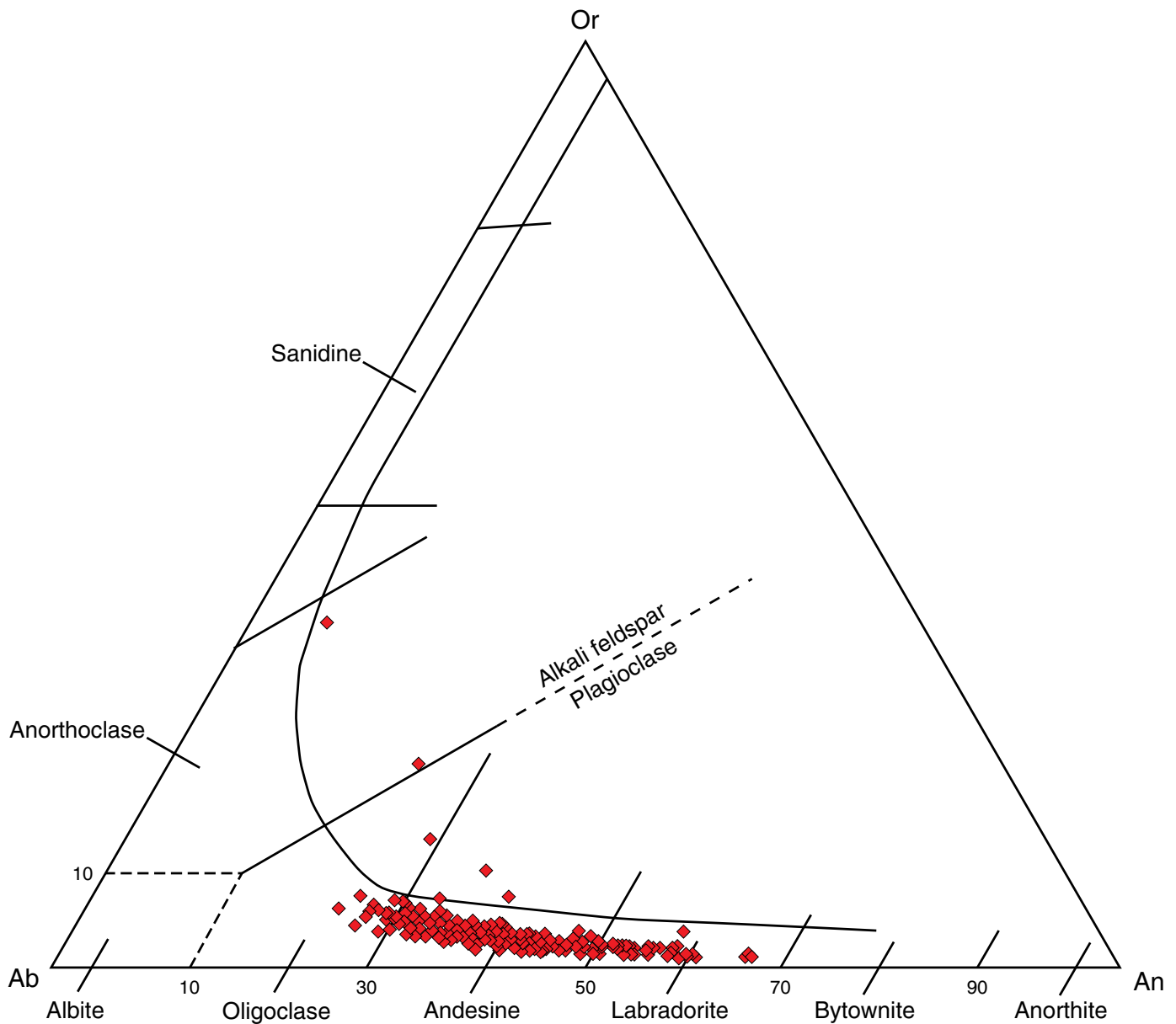


Figure 11. General classification of plagioclase from the NHVC. Modified after Correa-Tamayo (2009). Classification diagram originally taken and modified from Deer et al. (1966).

lization temperature calculation for the olivine was carried out, including several olivine–liquid geothermometers for hydrated or anhydrous conditions. A temperature range between 1219 and 925 °C was obtained, consistent with those obtained with the olivine–chromite geothermometer.

Clinopyroxene–liquid geothermobarometers were used to calculate clinopyroxene crystallization temperatures and pressures in equilibrium with the melt. A temperature range of 1221–971 °C was estimated, similar to values from the olivine–liquid geothermometer. The pressure values varied between 7.6 and 1.1 kbar, which correspond to depth values between approximately 23 and 3 km. With the clinopyroxene–liquid geo-

thermometer from Brizi et al. (2000), a range of temperatures between 943 and 856 °C was obtained.

With Cpx–Plag–Ol Thermobar, a temperature range between 1188 and 1109 °C was obtained for the crystallization of plagioclase in equilibrium with the melt under hydrated conditions. Pressures between 18 and 3 kbar indicated variations in the depth between 55 and 9 km. In part, these conditions of T and P are equivalent to those obtained with the olivine–liquid and clinopyroxene–liquid pairs.

Additionally, the amphibole geothermometer from Otten (1984) and the geobarometer of Johnson & Rutherford (1989) were used, with which temperature ranges between 940 and

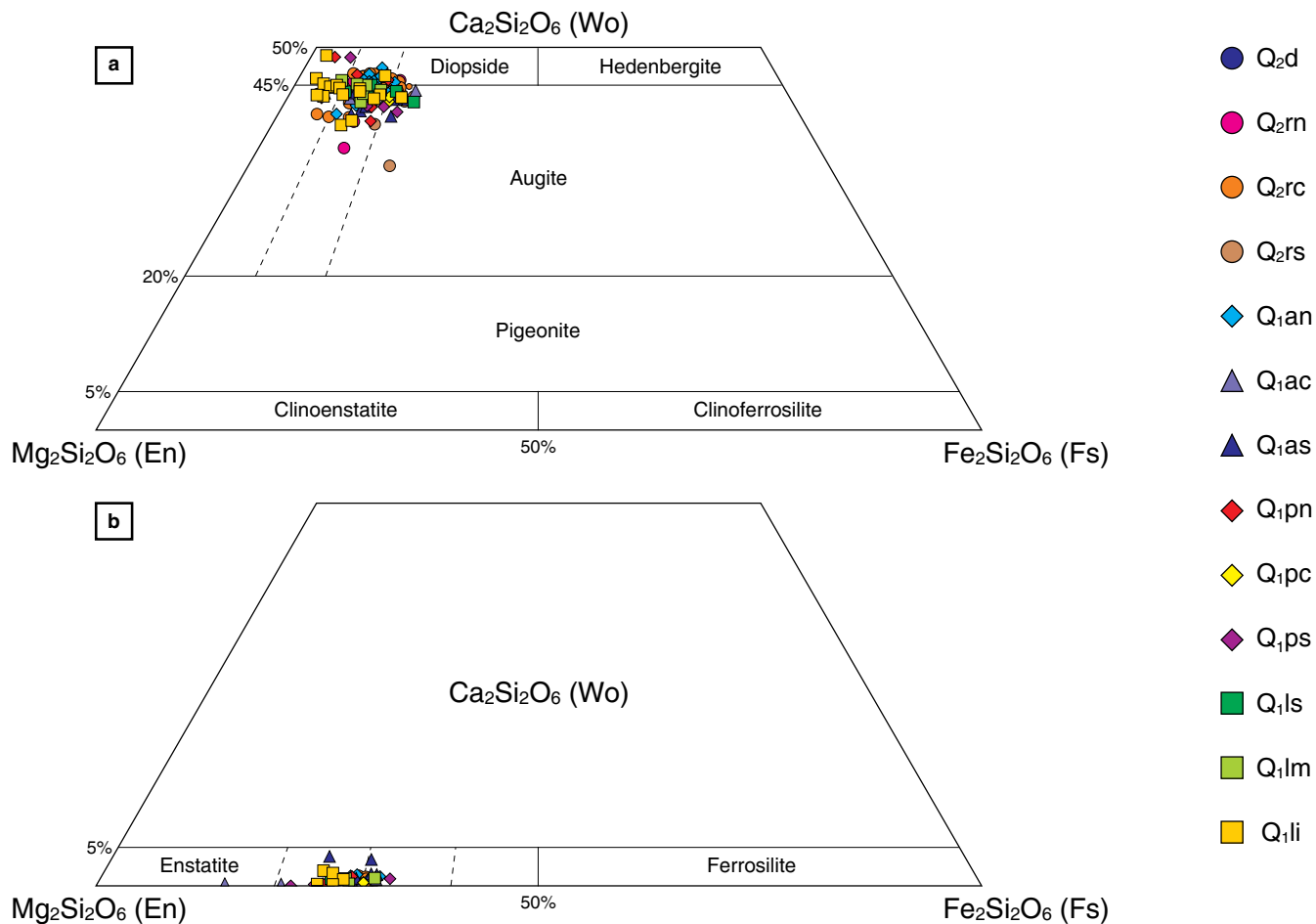


Figure 12. Classification of pyroxenes from the NHVC, in the diagram by Morimoto et al. (1988). **(a)** Clinopyroxenes. **(b)** Orthopyroxenes. Symbols as in Figure 10. Modified after Correa-Tamayo (2009).

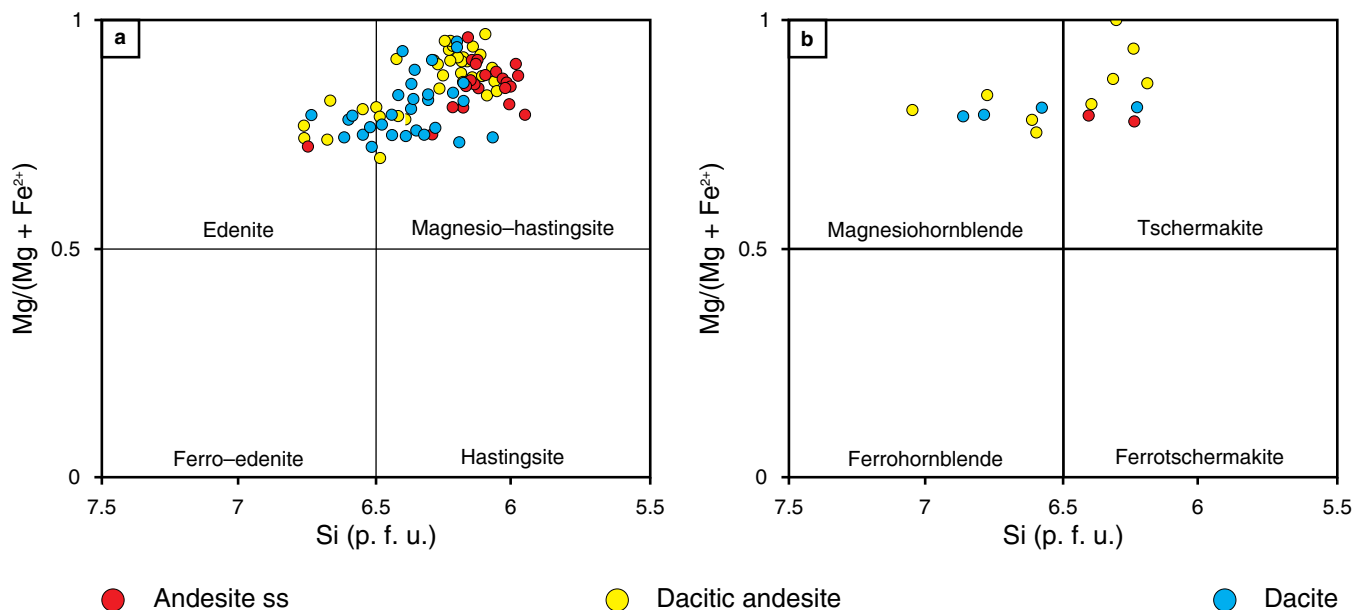


Figure 13. General classification of calcium amphiboles from the NHVC according to the nomenclature of Leake et al. (1997, 2004), which represents the compositional variations according to lithological type (andesite ss = red circles, dacitic andesite = yellow circles, and dacite = blue circles). **(a)** Series defined by the parameters of structural formula = $\text{Ti} < 0.50$, $(\text{Na} + \text{K})_A \geq 0.50$, $\text{Ca}_B \geq 1.50$, and $\text{Al}^{\text{vi}} < \text{Fe}^{3+}$. **(b)** Series defined by the parameters of structural formula = $\text{Ti} < 0.50$, $(\text{Na} + \text{K})_A < 0.50$, and $\text{Ca}_B \geq 1.50$. Modified after Correa-Tamayo (2009).

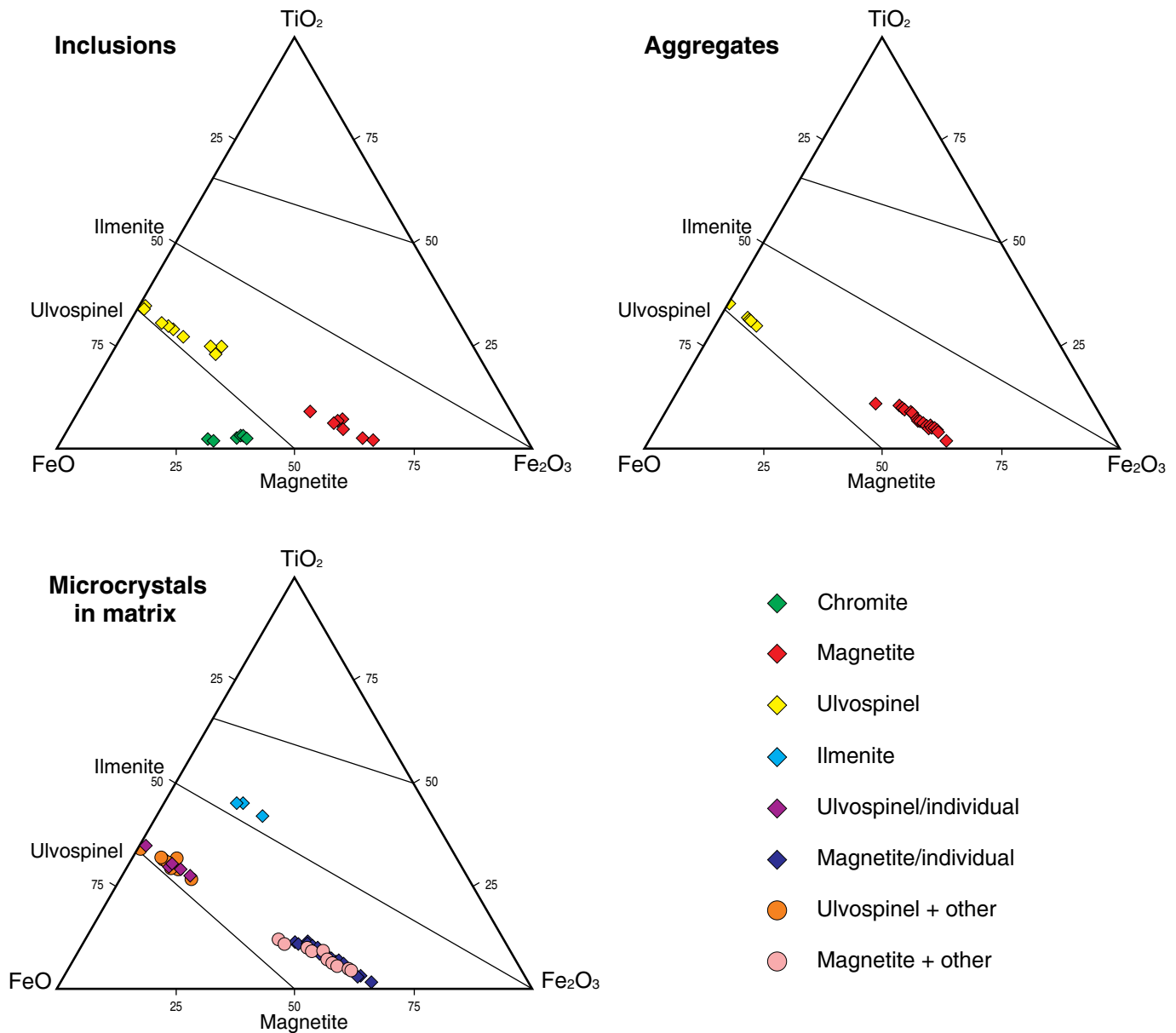


Figure 14. Classification and compositional variations in the Fe–Ti oxides present as inclusions, microcrystals in the matrix, or in microcrystalline aggregates in lavas from the NHVC. Modified after Correa–Tamayo (2009).

710 °C and pressures from 6.5 to 2.0 kbar were obtained, respectively. This pressure interval is equivalent to depths between 20 and 6 km. The temperatures are within the range of 950–650 °C, in which, according to Helz (1973), amphiboles of calc–alkaline magma crystallize.

3.6. Classification and Geochemical Affinity

The NHVC is composed of rocks of intermediate composition (andesites, 70% of the samples analyzed) to acid composition (dacites, 30%), with calc–alkaline affinity in the subalkaline series (Figure 17), SiO_2 content that varies from 57.96% to

65.37%, and medium K_2O content (1.44–2.91 %). According to the variations in SiO_2 content, three lithological types were identified: andesite ss (andesite sensu stricto, 57–60 %), dacitic andesite (60–63 %), and dacite (63–66 %).

The Q_{1ps} , Q_{1pc} , Q_{1as} , and Q_{1ac} units are specifically composed of dacitic andesites. In Q_{1an} , dacites predominate. In Q_{2rc} and Q_{2rn} , there are similar proportions of dacites and dacitic andesites, whereas in Q_{2rs} and Q_{2d} , andesites ss predominate. In these two units are the least differentiated rocks found to date in the NHVC. In the laguna de Páez sector, the geochemical variation follows the stratigraphic order: andesites ss in the Q_{1li} unit, dacitic andesites in Q_{1lm} , and finally dacites in Q_{1ls} .

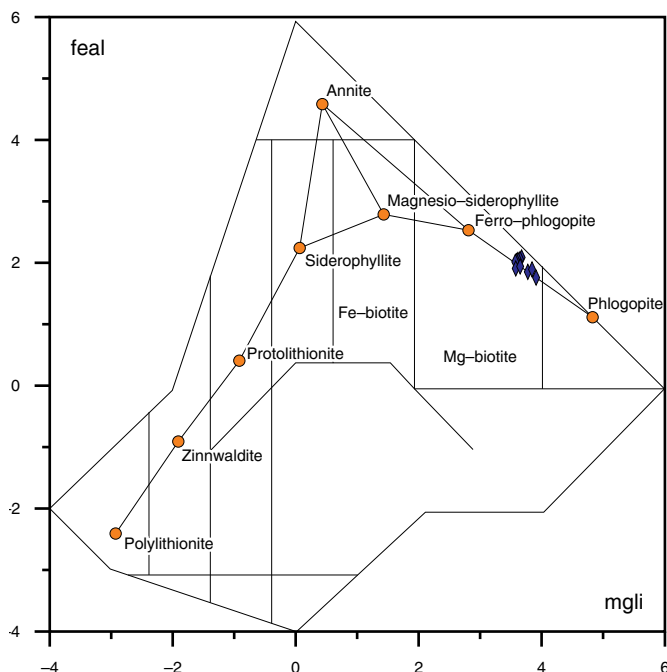


Figure 15. Classification of micas from the NHVC within the classification system PASP (phlogopite – annite / siderophyllite – polyolithionite), by Tischendorf et al. (2001), according to the variations in the contents of ferromagnesian minerals, aluminum, and lithium ($feal$ = total Fe + Mn + Ti + Al_{vi} – in octahedral position; $mgli$ = Mg + Li – in octahedral position). Circles = represent the “median” of composition representative of the eight main varieties of mica. Modified after Correa-Tamayo (2009).

3.7. Geochemical Variations in Major Elements and Trace Elements

The variations in major and trace elements with respect to magmatic evolution, that is, from andesites to dacites and as a function of the increase in SiO_2 (Figure 18), are evident in the decreases in the contents of major elements, except for K_2O and Na_2O . Equally, magmatic evolution is apparent from trends in the compatible elements (V, Sc, Co, and Zn), except for Cu, Cr, and Ni. In contrast, the contents of incompatible elements of the group LILEs (large ion lithophile elements, Rb, Ba, and Cs), except for Sr, or from the group HFSEs (high field strength elements, U, Th, Hf, Zr, and Pb) tend to be greater in more acid rocks, except for Y, Nb, and Ta. Al_2O_3 and P_2O_5 do not show any trend. This geochemical behavior is common in calc-alkaline rocks. The abundance of LREEs (light rare earth elements, La to Sm) is similar in andesites and dacites, whereas MREEs (middle rare earth elements, Eu to Tb) and HREEs (heavy rare earth elements, Dy to Lu) have moderate to low negative correlations with respect to the increase in SiO_2 .

The patterns of REE (Figure 19), normalized to chondrites (Nakamura, 1974), show high enrichment in LREEs with re-

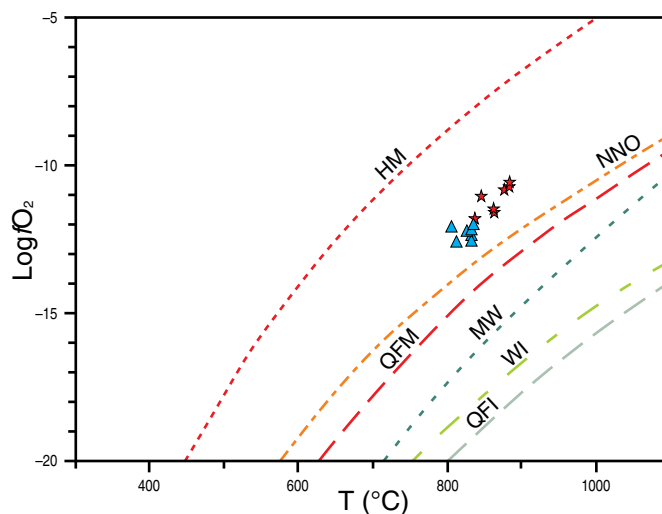


Figure 16. Diagram of temperature versus $\log fO_2$ for the two ilmenite–magnetite pairs of sample ACNH411 from Q_1li (pair of ilmenite–46/magnetite–35 = red star and pair of ilmenite–54/magnetite–35 = blue triangle). (REDOX reaction curves: HM = hematite–magnetite, NNO = Ni–NiO, QFM = quartz–fayalite–magnetite, MW = magnetite–wüstite, WI = wüstite–iron, and QFI = quartz–fayalite–iron). Modified after Correa-Tamayo (2009).

spect to HREEs, without significant anomalies. There is only a small positive anomaly in Tm (Tm/Tm^* average = 1.1).

The diagrams of incompatible trace elements normalized to the primitive mantle (Sun & McDonough, 1989) have very irregular patterns (Figure 20), with some parallel segments and fairly pronounced peaks and depressions. They are enriched in LILEs, HFSEs, and LREEs by more than 10 with respect to the primitive mantle, whereas enrichments in MREEs, HREEs, Y, and Ti show a decreasing trend from 10 to 1. There is a notable negative Nb–Ta anomaly ($Nb/Nb^* < 0.3$) and a positive Pb anomaly (Pb/Pb^* between 1.6 and 18.1). There are also some minor positive anomalies in Zr–Hf, Sr, La, and Tb and minor negative anomalies in Ce, Pr, Sm, and Ti–Dy.

In these multielemental diagrams, the patterns of the NHVC have some similarities with patterns of the averages of lower and upper continental crust (calculated by Rudnick & Gao, 2003). There are also similarities with patterns of rocks from other references considered, such as primitive andesites of continental arcs (Kelemen et al., 2007) and “Andean type” or typical andesite of a thick continental margin, calculated by Bailey (1981). There are also similarities with average andesite and dacite patterns of the Galeras Volcanic Complex and the Nevado del Ruiz Volcano and with average andesite and dacite patterns in Ecuador.

3.8. Adakitic Tendency

Some rocks of the NHVC present an adakitic tendency: low contents of Y (10 to 19 ppm) and HREEs (Yb 0.9 to 1.8 ppm),

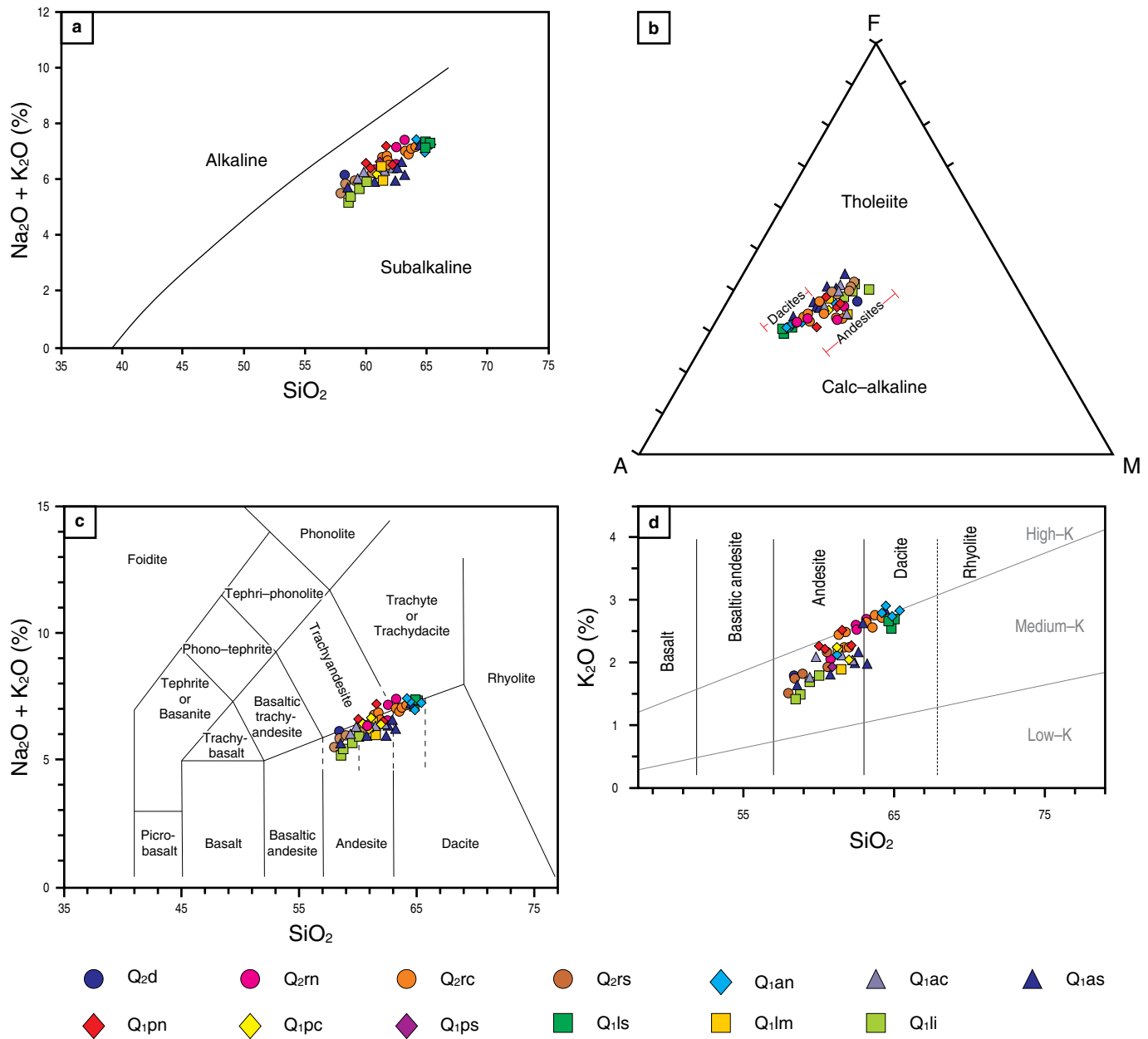


Figure 17. Classification and geochemical affinity diagrams for lavas from the NHVC. **(a)** SiO₂ vs. alkalis. **(b)** AFM (A = Na₂O + K₂O, F = Fe*O, M = MgO). **(c)** TAS. **(d)** SiO₂ vs. K₂O. (Symbols as in Figure 10). Modified after Correa-Tamayo (2009).

high concentrations of Sr (560 to 944 ppm), enrichment in LILEs and LREEs, and high values of Sr/Y (30 to 80) and La/Yb (13 to 32). In specific diagrams such as Y vs. Sr/Y and Yb_N vs. La/Yb_N (Figure 21), some samples plot in the adakitic affinity field, and others plot in the normal calc-alkaline field. This adakitic tendency is more evident in the most recent rocks that tend to have more dacitic compositions. On the other hand, the contents of Cs and Y in Q₁ac, Q₁an, Q₂rc, and Q₂rn are within the category of Cenozoic adakites following Drummond et al. (1996). Another typical aspect of adakitic rocks, from the petrological point of view, which is also seen in the NHVC, is the absence of associated basalt or basaltic andesites.

3.9. Petrogenetic Aspects

The Sr–Nd isotope composition is homogeneous (Table 5), with values of ⁸⁷Sr/⁸⁶Sr = 0.704140–0.704218 and ¹⁴³Nd/¹⁴⁴Nd = 0.512788–0.512833. These values are similar to those of other volcanoes in the NVZ, specifically from Ecuador (⁸⁷Sr/⁸⁶Sr = 0.7040–0.704543 and ¹⁴³Nd/¹⁴⁴Nd = 0.512617–0.51295; cf. Bourdon et al., 2002; Bryant et al., 2006; Samaniego et al., 2005) and Colombia (⁸⁷Sr/⁸⁶Sr = 0.704090–0.704770 and ¹⁴³Nd/¹⁴⁴Nd = 0.512728–0.512975; cf. James & Murcia, 1984; Marín-Cerón, 2007). This resemblance to the Sr–Nd isotope relationships of the NVZ indicates that the magmas in the NHVC

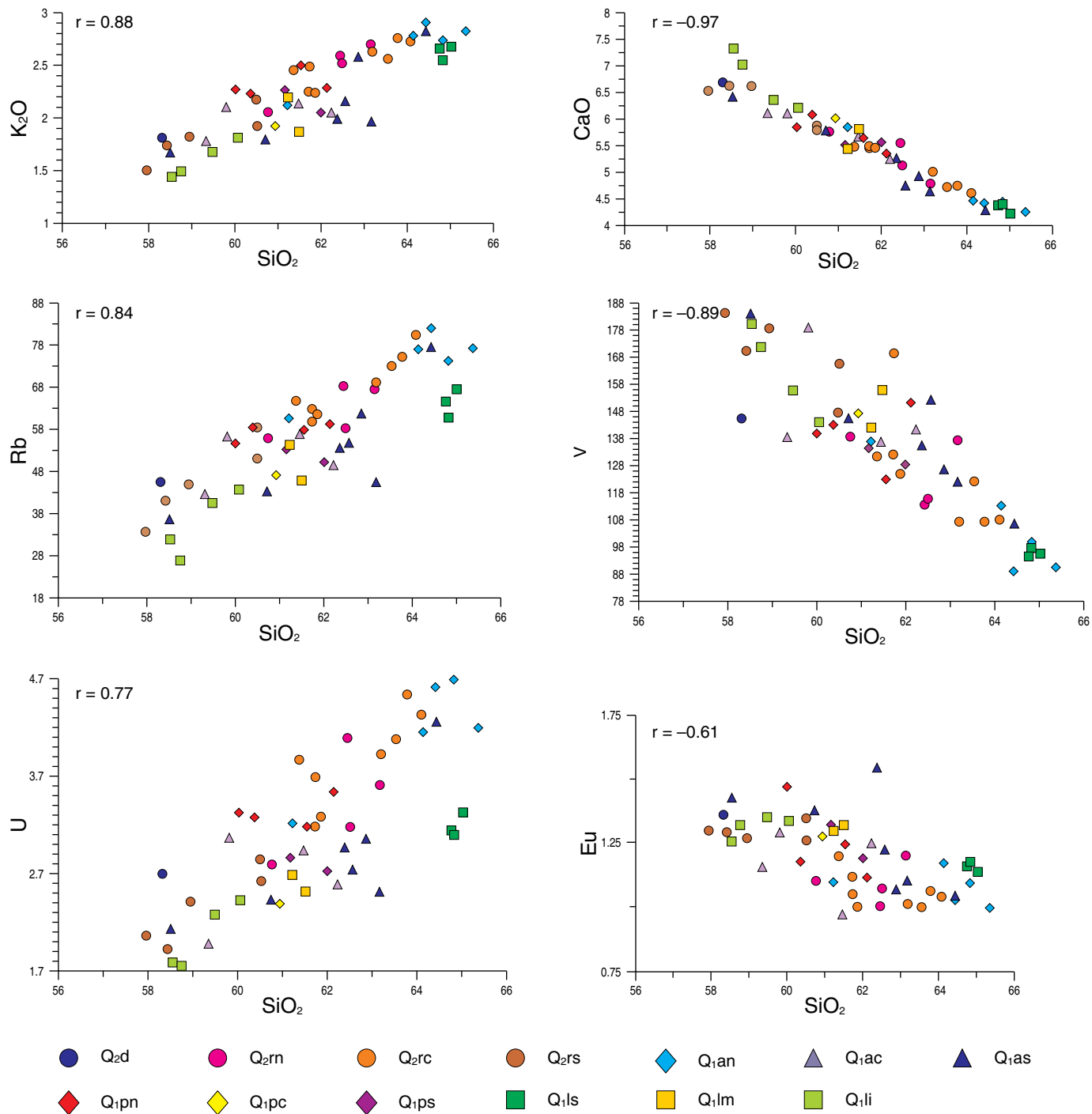


Figure 18. Geochemical variations of some major elements (wt %) and some trace elements (ppm) with SiO_2 content (wt %) projected in Harker diagrams, for lavas from the NHVC. (Symbols as in Figure 10). Modified after Correa-Tamayo (2009).

were generated by partial fusion of a mantle source, similar to most of the typical andesites of the arc, and did not experience significant crustal contamination, unlike the andesites of the central Andes (James & Murcia, 1984). For Thorpe et al. (1984), these isotopic characteristics in magmas of the NVZ are consistent with petrogenesis from mantle that is enriched in radiogenic Sr derived from the subducted plate, with little to no

contamination by continental crust, which is reflected in mantle trends (mantle array).

In the $^{87}\text{Sr}/^{86}\text{Sr}$ vs. $^{143}\text{Nd}/^{144}\text{Nd}$ diagram (Figure 22), samples from the NHVC, the Galeras Volcanic Complex, and Nevado del Ruiz Volcano plot within or very near the field of the NVZ. When compared to materials of mantle origin (MORB and OIB of the East Pacific Rise, Galápagos spreading center,

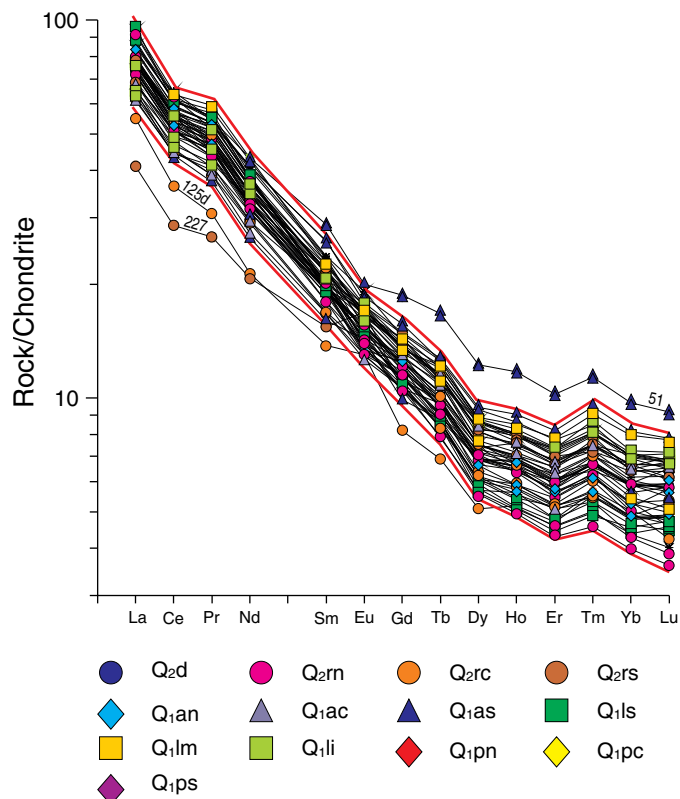


Figure 19. Diagram of REE normalized to chondrites of Nakamura (1974) for lavas from the NHVC. (Symbols as in Figure 10). Modified after Correa-Tamayo (2009).

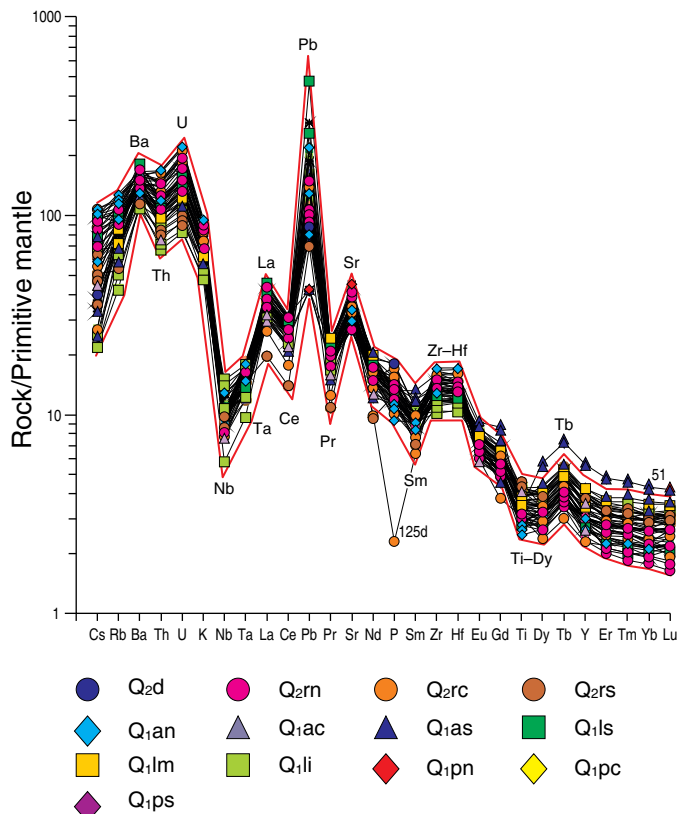


Figure 20. Multielement diagrams of incompatible trace elements normalized to the primitive mantle according to Sun & McDonough (1989) for lavas from the NHVC. (Symbols as in Figure 10). Modified after Correa-Tamayo (2009).

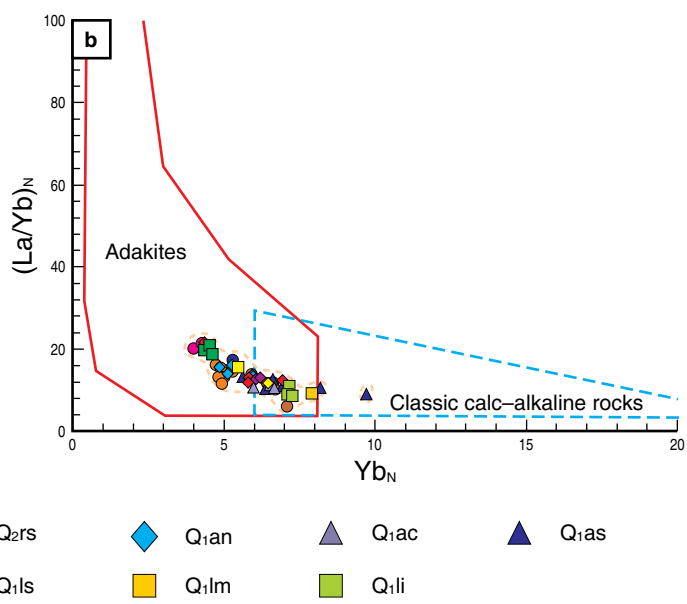
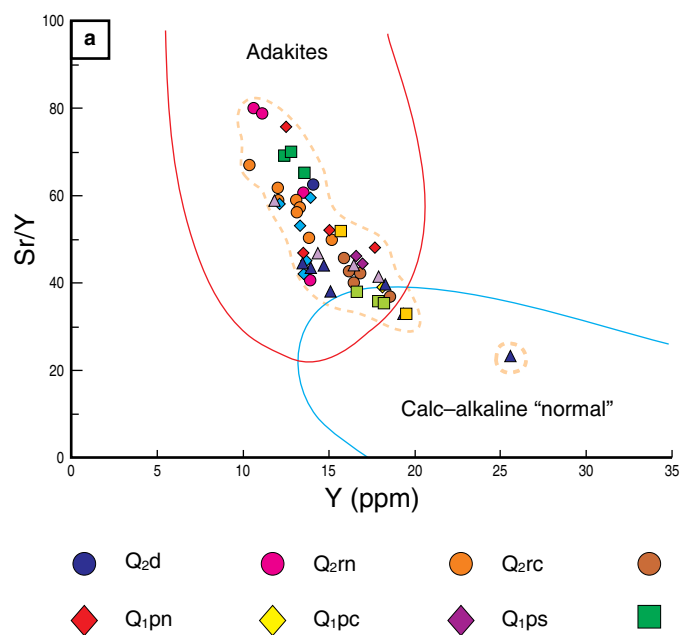


Figure 21. Diagrams of discrimination between adakites and “normal” calc-alkaline rocks in which representative samples of the NHVC have been projected. **(a)** Y vs. Sr/Y (inspired by diagram in Defant & Drummond, 1990). **(b)** Yb_N vs. (La/Yb)_N (inspired by diagram in Martin, 1986, 1999). (Symbols as in Figure 10). Modified after Correa-Tamayo (2009).

Table 5. Rb–Sr and Sm–Nd isotope relationships in five representative samples from NHVC* lavas.

Volcano–stratigraphic unit	Sample	Classification		$^{87}\text{Sr}/^{86}\text{Sr}$	$^{143}\text{Nd}/^{144}\text{Nd}$
		Petrographic	Geochemical		
Q _{rn}	BPNH105	Amphibole + clinopyroxene andesite	Dacite	0.704167	0.512809
Q _{an}	ACNH203	Amphibole–clinopyroxene andesite	Dacite	0.70416	0.512788
Q _{pn}	ACNH401	Clinopyroxene + orthopyroxene andesite	Dacitic andesite	0.70414	0.512794
Q _{ls}	ACNH407	Amphibole–clinopyroxene andesite	Dacite	0.704218	0.512823
Q _{li}	BPNH307	Clinopyroxene + orthopyroxene andesite	Andesite ss	0.704171	0.512833

Note: The samples were analyzed in the mass spectrometer Micromass VG Sector 54 (TIMS) of the Centro de Geocronología y Geoquímica Isotópica de la Universidad Complutense de Madrid. The analytical errors refer to two standard deviations and are 1% in the $^{87}\text{Rb}/^{86}\text{Sr}$ ratio, 0.01% in the $^{87}\text{Sr}/^{86}\text{Sr}$ ratio, 0.1% in the $^{147}\text{Sm}/^{144}\text{Nd}$ ratio, and 0.006% in the $^{143}\text{Nd}/^{144}\text{Nd}$ ratio.

(ss) sensu stricto.

*Modified after Correa–Tamayo (2009).

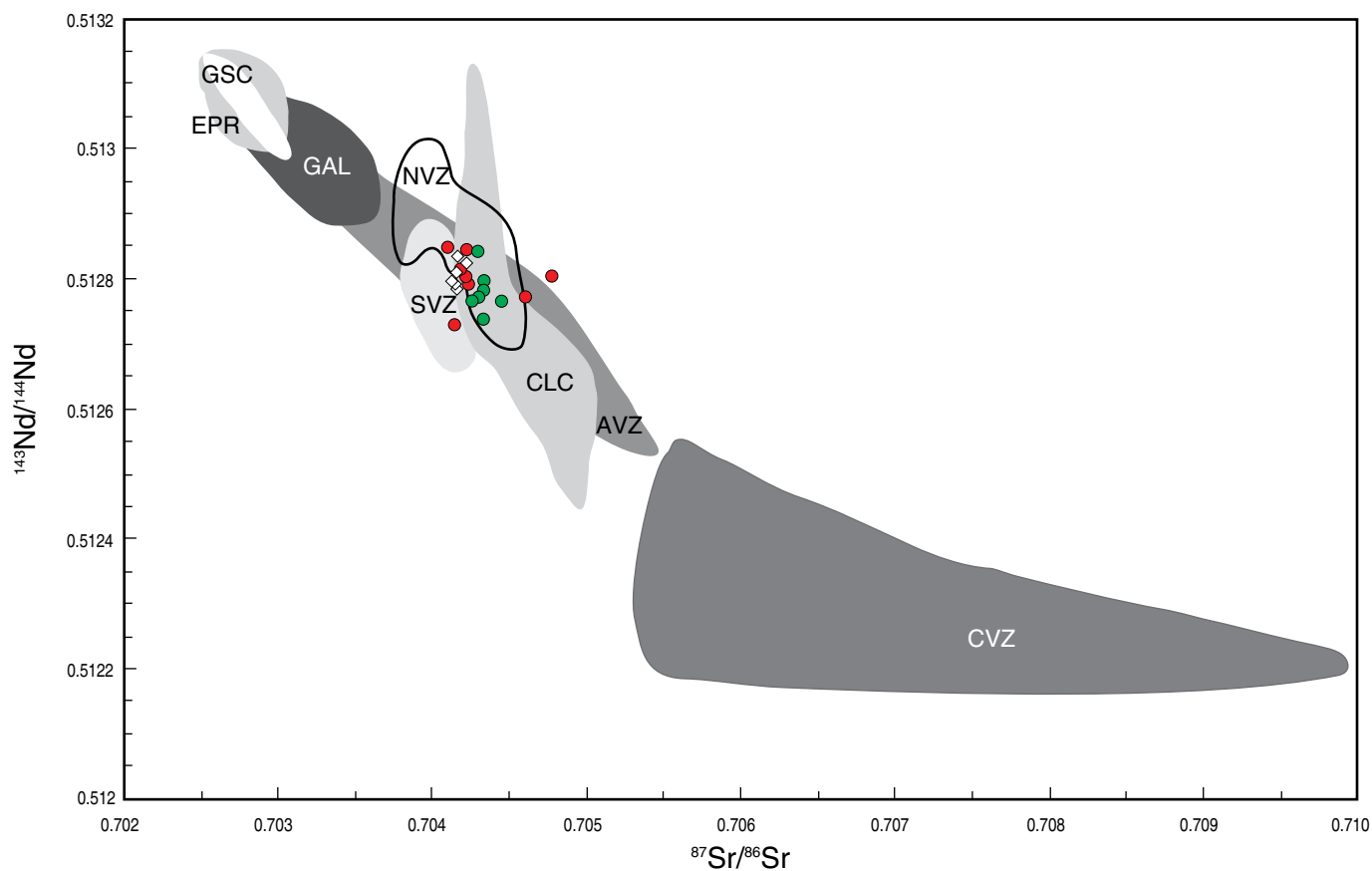


Figure 22. Diagram $^{87}\text{Sr}/^{86}\text{Sr}$ vs. $^{143}\text{Nd}/^{144}\text{Nd}$ for NHVC rocks (white rhombus), compared with fields of Sr–Nd isotope ratios from other zones, as defined by Samaniego et al. (2005): (GSC) Galápagos spreading center, (EPR) East Pacific Rise, (GAL) Galápagos Islands, (NVZ) North Volcanic Zone of the Andes, (SVZ) South Volcanic Zone of the Andes, (AVZ) Austral Volcanic Zone of the Andes, (CVZ) Central Volcanic Zone of the Andes, and (CLC) xenoliths of lower continental crust in SW Colombia. To compare, some samples from the Colombian volcanoes Nevado del Ruiz (green circle) and Galeras (red circle), whose isotopic data were reported by James & Murcia (1984), are also represented. Modified after Correa–Tamayo (2009).

and Galápagos Islands hotspot), it is evident that the samples from the NHVC are within the mantle array with low values of $^{87}\text{Sr}/^{86}\text{Sr}$ and high values of $^{143}\text{Nd}/^{144}\text{Nd}$, indicating that the magma was possibly generated by partial fusion of the mantle source with little crustal participation. In addition, the homogeneous isotopic relationships reveal that magmatic evolution was not significantly affected by the participation of contaminants derived from the continental crust.

The enrichments in Sr, K, Rb, Ba, and Th with respect to MORB in the less differentiated andesites of the NHVC (Figure 23) would reflect, according to Pearce (1983), the possible participation of subduction zone components in petrogenesis. In contrast, the depletions in Ta, Nb, Ce, P, Zr, Hf, Sm, Ti, Y, and Yb are perhaps caused by fractional crystallization and possible participation of enriched upper mantle. Likewise, the high enrichment in Th and relative enrichment in Nb of these less differentiated andesites, with respect to MORB, indicates a possible mantle source enriched in Th and Nb. This remarkable enrichment in Th may be caused by components coming from the subduction zone (Thorpe et al., 1984).

The behavior of the trace elements (Figure 24) permits the interpretation that the petrogenetic processes determining magmatic evolution in the NHVC, from andesites ss to dacites, have primarily been partial melting and fractional crystallization. We cannot eliminate contamination or assimilation and magma mixing, possibly caused by magma recharge, judging by certain textural evidence and compositional variations and the possibility of magmatic differentiation in an open system.

From the behavior of the major elements, we conclude that the fractional crystallization process has been homogeneous and that the following minerals have participated in more or less similar proportions: plagioclase, clinopyroxene, orthopyroxene, amphibole, and Fe–Ti oxides (magnetite). As crystallization progresses, reflected in the increase in the evolution index ($\% \text{SiO}_2$), Al_2O_3 decreases due to extraction of mineral phases such as plagioclase. Additionally, some of the mafic minerals participated in the decrease in MgO. Finally, the decrease in TiO_2 implies the participation of phases rich in this element, such as amphibole or some of the opaque minerals (Figure 25).

Using the XLFrac program designed by Stormer & Nicholls (1978), 180 mathematical models of fractional crystallization were calculated through mass balance with the least squares method. The models were based on the contents of major elements, selecting in each unit the most extreme compositions, that is, the least differentiated andesite and the most acid dacite, using mineral chemistry data that correspond to the mean compositions of the nuclei of the phenocrysts or microphenocrysts. Among the models calculated, those with best fits to the actual mineralogical composition of the rocks or those with more geological coherence and the lowest residual values were selected. The best models always involve the participation of plagioclase (usually more than 50% of the minerals extracted) and the participation

of magnetite (in percentages between 4% and 9%), accompanied by clinopyroxene and/or amphibole in variable proportions (between 10% and 20%). These results agree with deductions from the contents of major elements in graphic form.

Fractional crystallization models were calculated using the contents of trace elements, taking into account the degree of crystallization (calculated in models with major elements), the percentages of participation of each mineral phase (obtained in the previous models), and partition coefficients (K_D) between minerals and andesitic and dacitic liquids (taken from Rollinson, 1993). With these calculations, it was established that the Rayleigh fractional crystallization model (CF–Ra) fits better than the equilibrium fractional crystallization model (CF–eq). It is confirmed that the best calculated models always involve the participation of plagioclase + clinopyroxene + magnetite, usually with amphibole and occasionally orthopyroxene.

4. Discussion

Some conclusions of de Silva & Francis (1991), in their research on central Andes volcanoes, are extrapolated to the NHVC. In the central Andes, there are three types of volcanoes: (1) those that have been affected by glacial action and have not experienced any volcanic activity after the Last Glaciation; (2) volcanoes that show no evidence of having undergone glaciations and whose surfaces seem to have been formed in post-glacial periods; and (3) hybrids between these two extremes, which exhibit both glacial features (valleys, moraines, etc.) and juvenile volcanic features, indicating complex histories. This intermediate situation corresponds to the NHVC. In addition, for these authors, the moraines constitute very consistent time markers: the moraines and glacial valleys at elevations as low as 4300 masl formed during the last great glacial retreat, 11 000 to 10 000 years BP, whereas the moraines that formed during the Little Ice Age spread slightly below the boundaries of the current ice sheet.

By comparing the NHVC with the model proposed by Short (1986) for the erosive evolution of volcanoes in five stages (from stage 1, young cones without evidence of glacial action or erosion in general and with clearly recognizable and well-preserved volcanic features, to stage 5, with barely recognizable volcanic evidence, very degraded and smooth relief, and radial symmetry as the main sign of the volcanic origin), we conclude that the PHS edifice presents features similar to those of stage 5 of the model of morphological evolution, whereas the amounts of relief on the AHS and RHS correspond to stages 4, 3, and 2.

According to van der Wiel (1991), four volcanoclastic terraces along the Páez and La Plata Rivers that were generated by volcanic debris flows or volcanoclastic deposits, whose source of material was the NHVC, were formed at 1 Ma based on four K–Ar dates in samples of volcanic rock fragments taken from these deposits, which produced an age of $1.1 \pm$

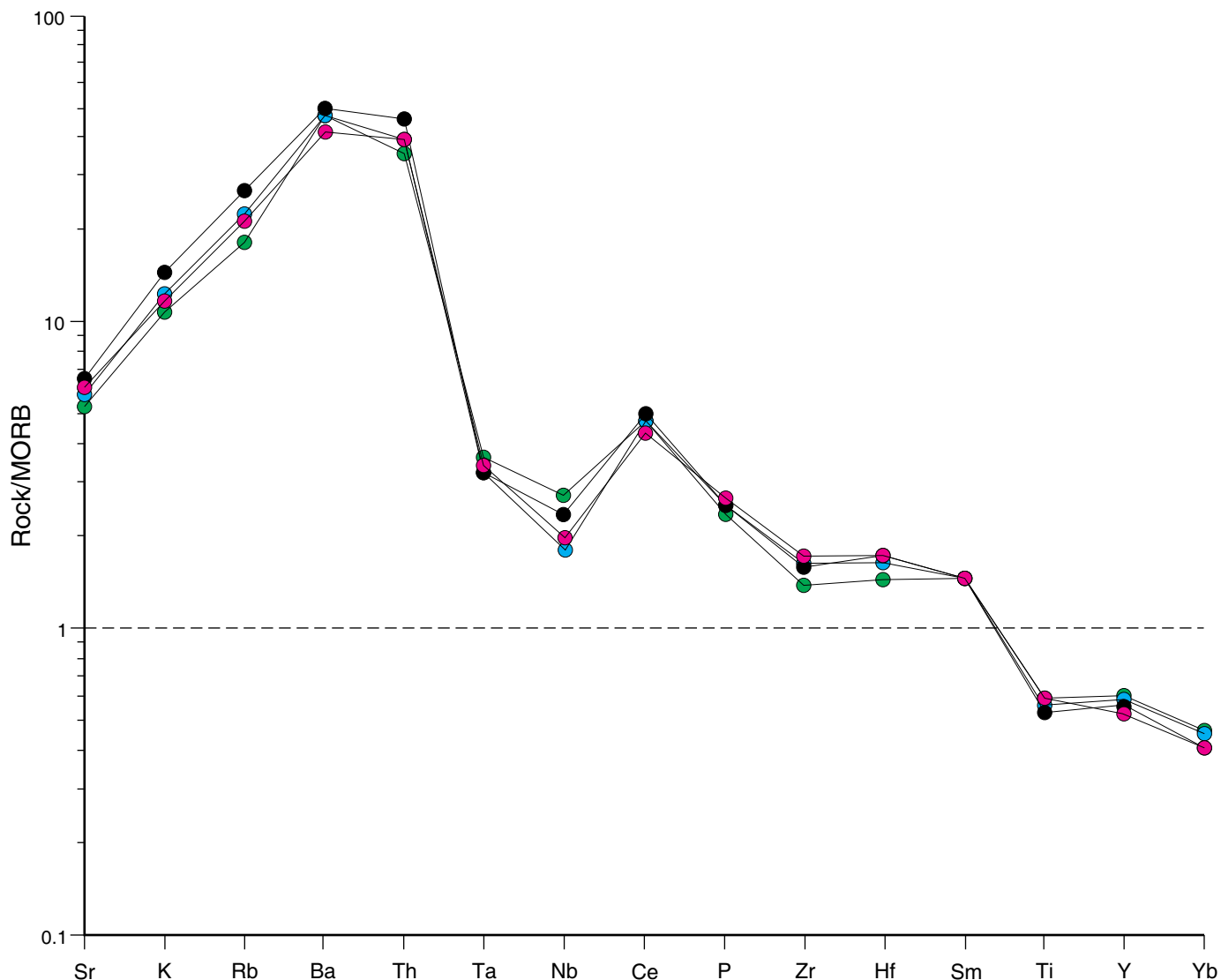


Figure 23. Geochemical patterns of less differentiated andesites from the NHVC, normalized to MORB. Q1li: green circles, PHS andesites: black circles, AHS andesites: blue circles, and RHS andesites: pink circles. Selection and distribution of incompatible elements on the ordinate axis; scale of graph and MORB normalization values according to Pearce (1983). Modified after Correa-Tamayo (2009).

0.2 Ma. This age supports the idea that the NHVC has been active for at least 1 Ma.

As indicated before, the geochemical behavior of rocks from the NHVC places them in the calc-alkaline field with medium to high K contents that are typical of an active continental margin. In particular, the patterns of REE are typical of orogenic andesites, in which, according to Bailey (1981) and Gill (1981), there is a distinctive marked fractionation in the patterns of REE, an absence of pronounced negative Eu anomalies, a negative inflection in Ce and the concave upward slope reflected in the Dy to Er ratio.

In comparing the behavior of REE in the average andesites of the NHVC with two similar references, some peculiarities arise (Figure 26). This andesite presents minor enrichments in REE, mainly in LREEs, with respect to the “Andean type” an-

desite, which for Bailey (1981) characterizes a thick continental margin environment, and corresponds to the median of several Andean andesites typical of Perú and northern Chile or the Central Volcanic Zone (CVZ) of the Andes. In contrast, with respect to the average of 32 samples of andesites from 12 volcanoes in Ecuador as a representation of the NVZ of the Andes (data taken from Bryant et al., 2006), the NHVC has notably higher enrichments in LREEs and MREEs. The difference in enrichments in HREEs between volcanoes in Ecuador and the NHVC is smaller. By comparison to the full range of samples of the NHVC, it is apparent that some rocks follow patterns closer to those of the CVZ, whereas others are similar to rocks from Ecuadorian volcanoes.

Several of the main characteristics of the behavior of trace elements in rocks of the NHVC reflect some typical crustal features. According to Kelemen et al. (2007), these features

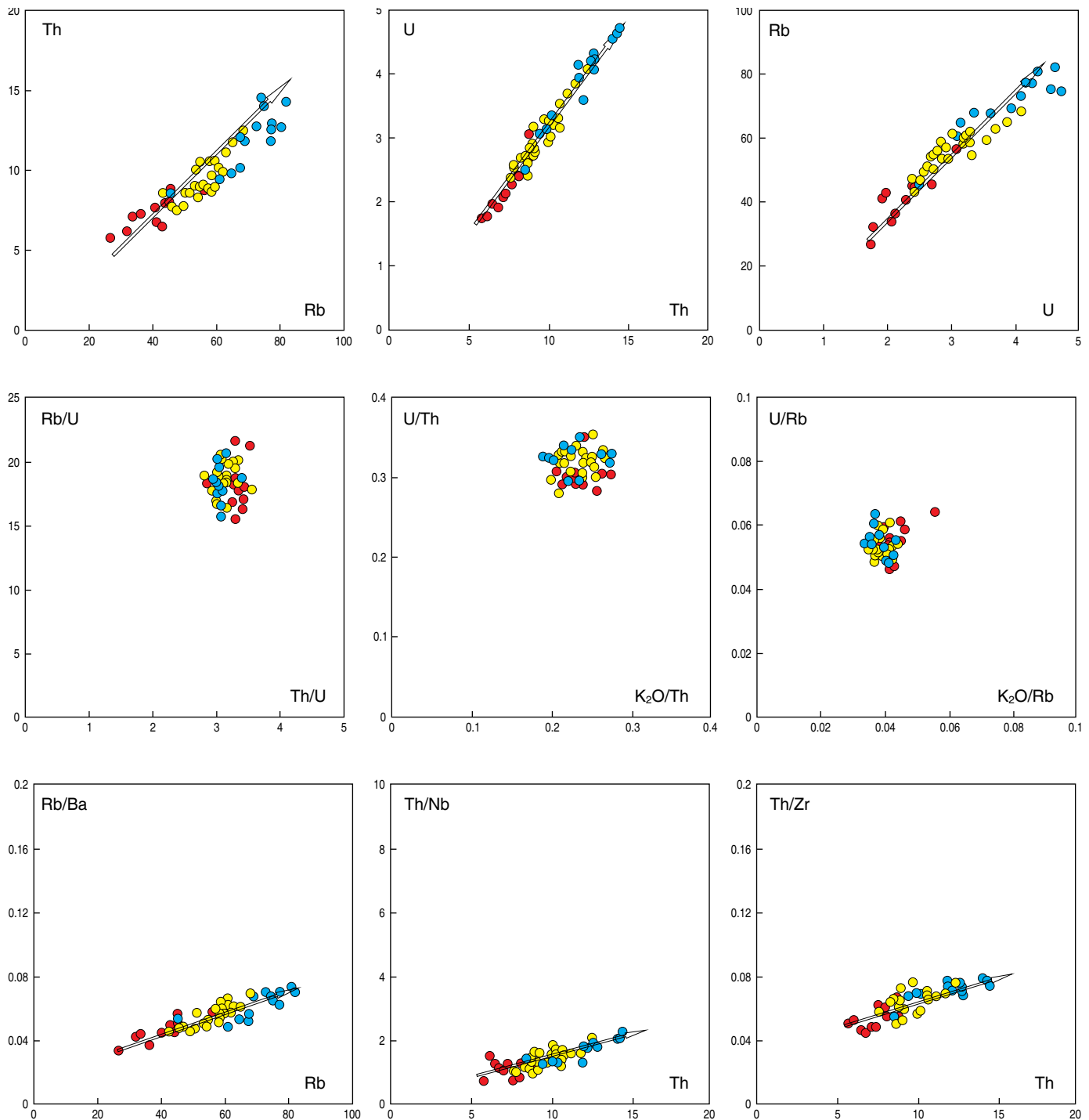


Figure 24. Relationships between trace elements (incompatible and/or moderately incompatible), which allow discrimination of the type of petrogenetic process that is predominant in the magmatic evolution of the NHVC. Andesite ss: red circles, dacitic andesite: yellow circles, and dacite: blue circles. Modified after Correa-Tamayo (2009).

are high enrichment in incompatible elements (LILEs + Th–U) with respect to mantle material, lower enrichments in HREEs and Y; a marked negative anomaly in Nb–Ta, a notable positive anomaly in Pb, and minor anomalies in Ti–Dy and Zr–Hf.

More than one petrogenetic model for rocks with adakitic tendency has been proposed. Castillo (2006) compiled and syn-

thesized several of these models, considering that they allow the participation of a component of basalt metamorphosed to eclogite facies as a magmatic source in a subduction environment and that geochemical heterogeneity results from the participation of other magma generation and differentiation mechanisms (Atherton & Petford, 1996; Bryant et al., 2006; Defant & Drum-

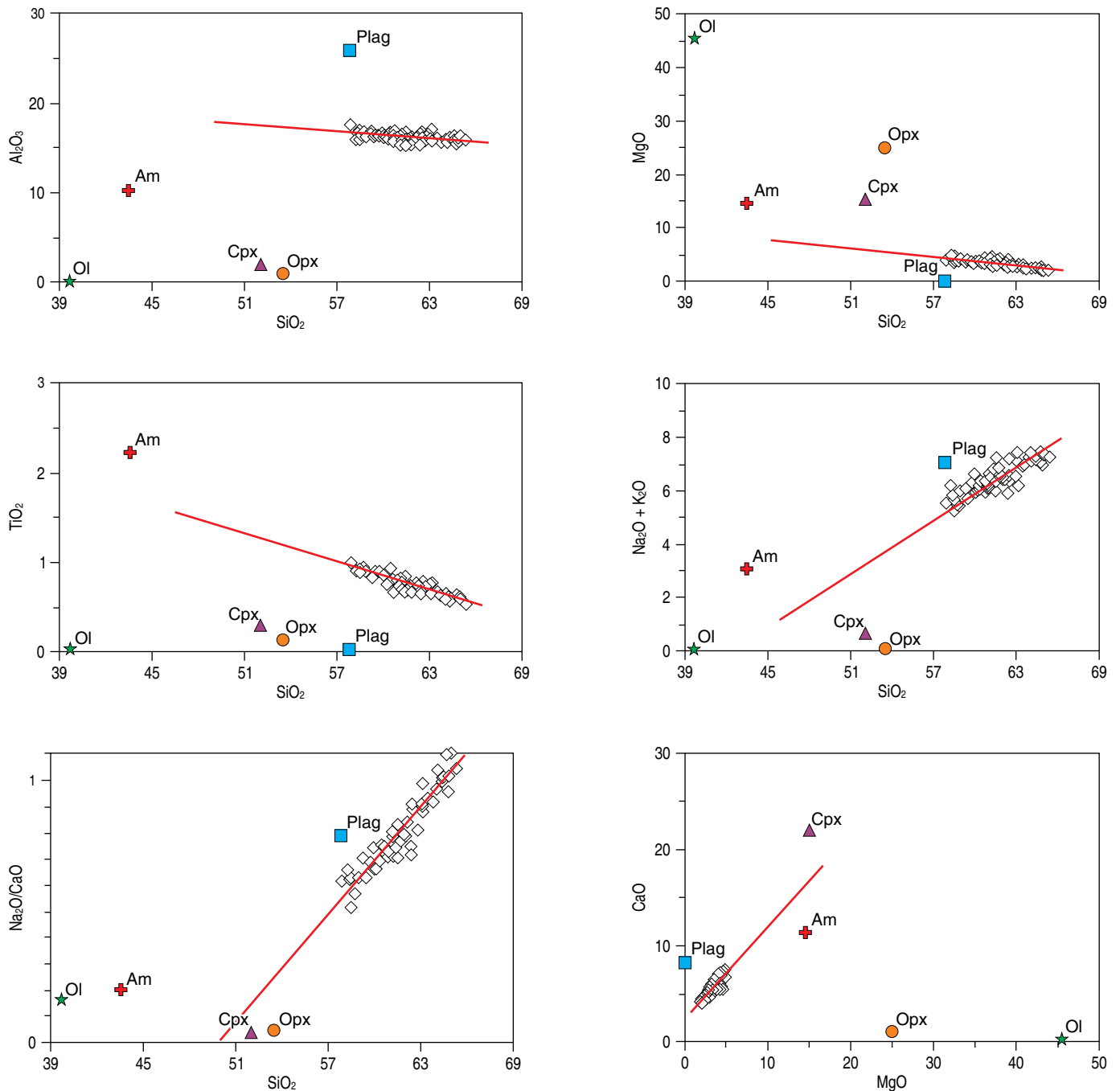


Figure 25. Binary diagrams of relationships between major elements (wt %) to determine the participation of each mineral phase in fractional crystallization in lavas from the NHVC. Representative samples of the NHVC: white rhombus, average composition of the plagioclases analyzed: blue quadrate, average composition of the clinopyroxenes analyzed: violet triangle, average composition of the amphiboles analyzed: red cross, average composition of the orthopyroxenes analyzed: orange circle, and average composition of the olivines analyzed: green star. Modified after Correa-Tamayo (2009).

mond, 1990; Drummond & Defant, 1990; Drummond et al., 1996; Martin, 1986, 1999; Maury et al., 1996). Four main models have been proposed: (1) partial fusion of subducted young oceanic crust, as proposed by Defant & Drummond (1990), for typical adakite; (2) partial fusion of an asthenospheric wedge (peridotitic) that was previously metasomatized by liquids and/

or melts from the subduction plate, where basalts rich in Nb, andesites high in Mg, or rocks with adakitic tendency are generated through this process; (3) deep fractional crystallization and assimilation of the upper continental crust to produce adakitic rocks, while the parental magmas were generated by mantle melting, previously metasomatized as in model 2; and (4) par-

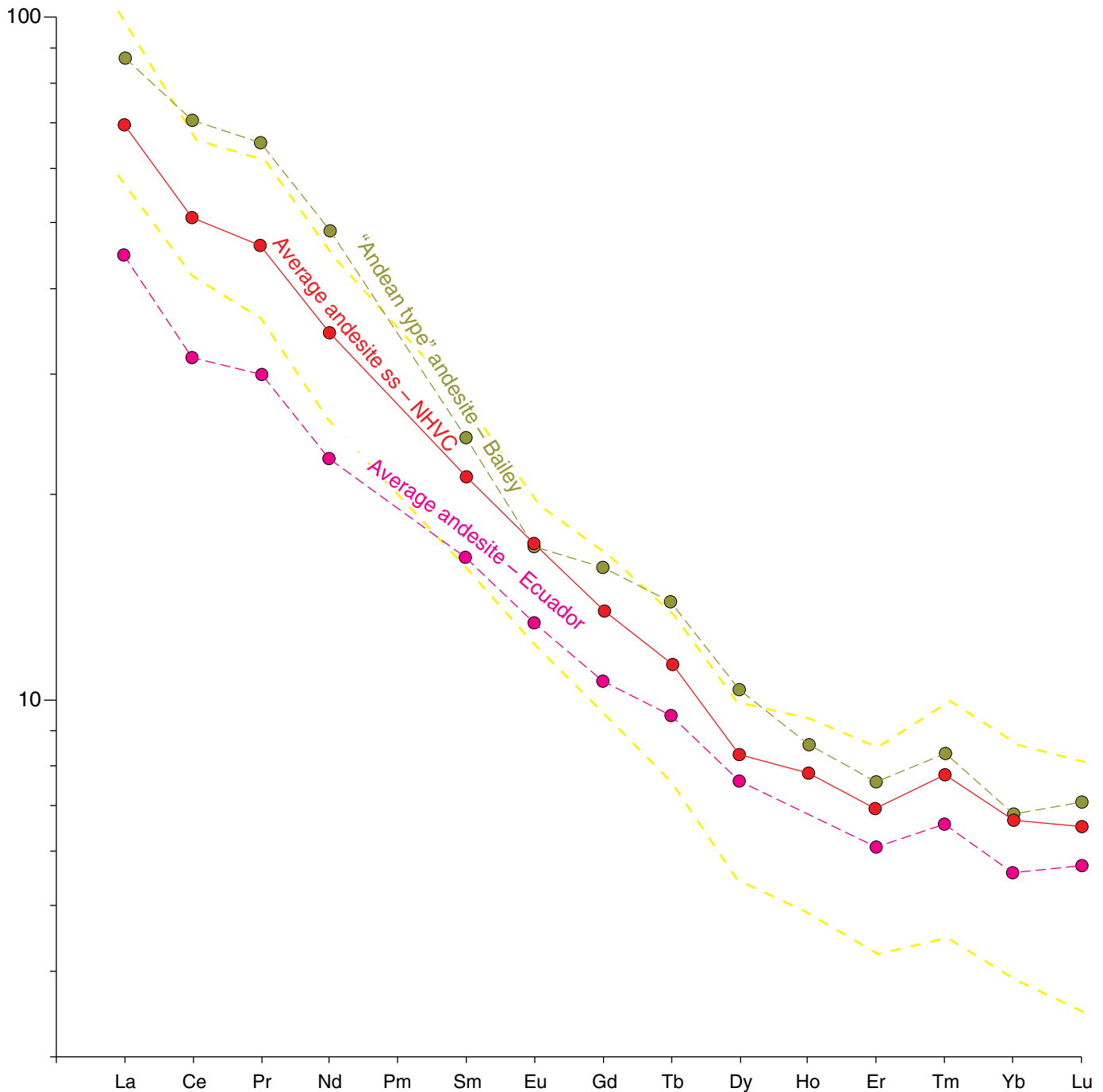


Figure 26. Comparison of REE patterns normalized to chondrites of Nakamura (1974) between average andesite ss of the NHVC (red circles and line), average andesite from 12 volcanic centers in Ecuador (data taken from Bryant et al., 2006; fuchsia circles and line), and “Andean type” andesite (Bailey, 1981; green circles and line), which corresponds to values of the median that represents the typical andesite of the central Andes, Perú, and northern Chile. The yellow dotted lines correspond to the range of variation for NHVC lavas. Modified after Correa-Tamayo (2009).

tial fusion of lower continental crust, accreted under thick orogenic belts (>50 km). A fifth mechanism is crustal delamination, in which the delaminated lower crust can sink into the relatively warm mantle and undergo partial fusion.

Although the adakitic tendency in some samples from the NHVC could lead to an interpretation of magma evolution by

partial melting of subducted oceanic crust, there are clear arguments against this: the geochemical variations exclude the origin of magma by partial melting of a mantle wedge; the depth of the Benioff zone, between 140 and 200 km (Gutscher et al., 1999; James & Murcia, 1984; Pennington, 1981), is greater than the depth necessary for the “adakite window”, between 75 and

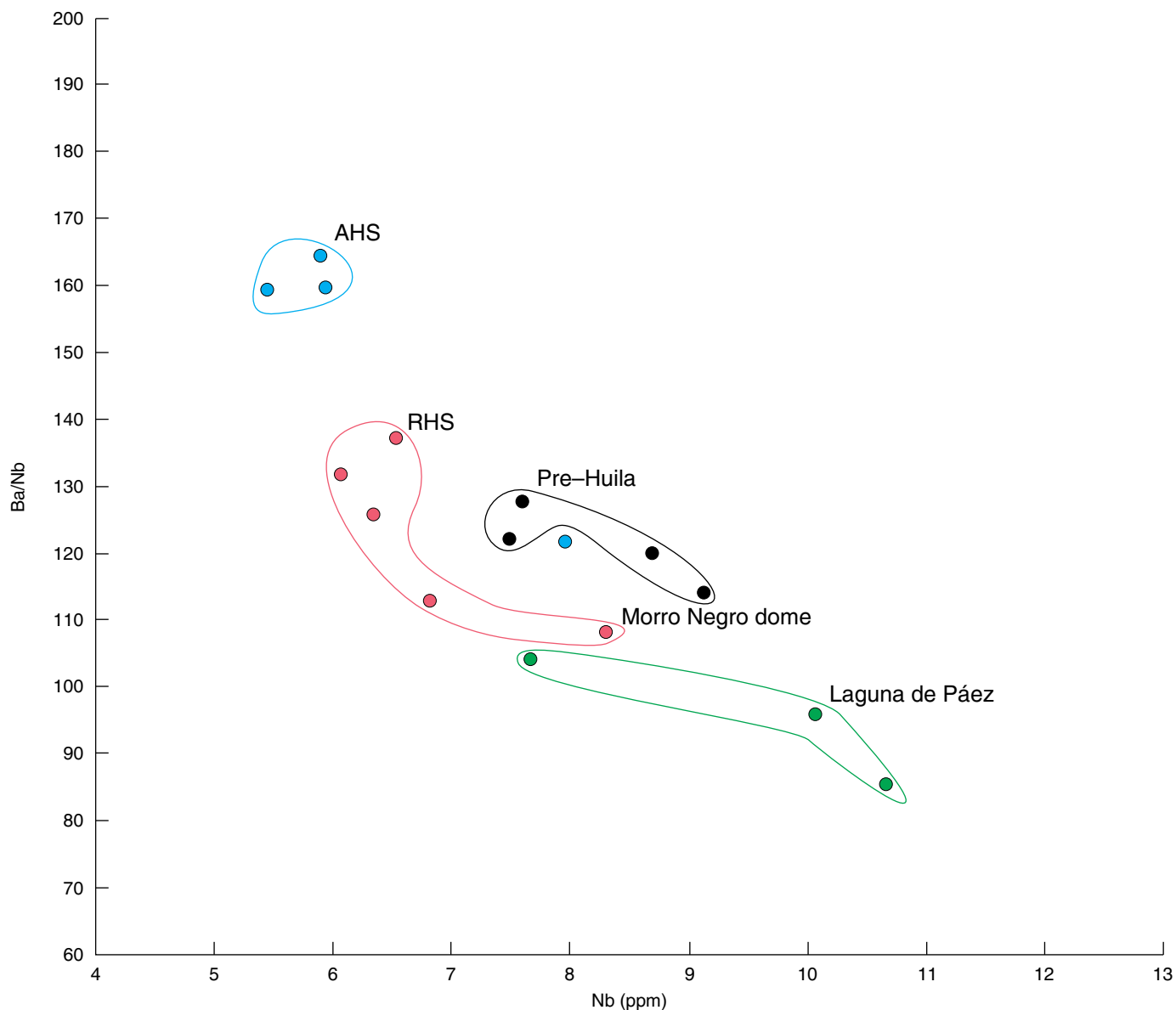


Figure 27. Diagram of geochemical variations between Nb vs. Ba/Nb for the less differentiated andesites from the NHVC: (AHS) Ancient Huila Stage and (RHS) Recent Huila Stage. Modified after Correa-Tamayo (2009).

85 km (Drummond & Defant, 1990); and there is no positive correlation between Ba/Nb and Nb (Figure 27) from the adakitic magma (Bourdon et al., 2002). Furthermore, in the NHVC, the $^{87}\text{Sr}/^{86}\text{Sr}$ relationships are slightly greater than the range that corresponds to typical Cenozoic adakites, but they are lower than those of volcanic rocks from the CVZ of the Andes.

5. Conclusions

The NHVC has evolved since 1.5 Ma when its eruptive history began, which is reflected both in its geomorphological features and in its stratigraphic and petrographic characteristics and compositional variations. These characteristics, in turn, indicate equally complex magmatic evolution and petrogenesis.

From geomorphological analyses, compositional variation can be deduced from less viscous magmas with intermediate composition to more viscous magmas with more acid composition. The estimated volume (120 to 135 km³) and the slope values (13° to 22°) correspond to calc-alkaline volcanoes (Cas & Wright, 1987) with intermediate to acid composition (Short 1986).

The eruptive history includes three stages, each with a different duration: the PHS started in the early Pleistocene and continued during the rest of the Pleistocene; the AHS began 100 000 years ago and lasted 90 000 years in the Late Pleistocene; and when the Last Glaciation ended 11 000–10 000 years ago, the RHS began and was prolonged into the Holocene.

The predominant lava products emitted during these stages of NHVC construction are grouped into 13 volcano-stratigraphic

ic units. Two–pyroxene andesites, clinopyroxene andesites, amphibole–clinopyroxene andesites, amphibole andesites, and others have been identified. The rocks with the highest amphibole contents are those that correspond to the RHS and those from Q_{2d}, whereas in rocks of the PHS, the orthopyroxene contents are higher. The complex eruptive history includes at least one episode of gravitational, not magmatic, collapse that generated a succession of debris avalanches and associated debris flows (Q_{1ae}) in the Late Pleistocene.

The geochemical variations are evident both in terms of the development of the eruptive history of the NHVC and in the geographical position of the units. Rocks belonging to units of the PHS and to Q_{1as} and Q_{1ac} are mainly composed of dacitic andesites, whereas in Q_{1an}, dacites predominate. In Q_{2rc} and Q_{2rn}, there are dacites and dacitic andesites in similar proportions; in Q_{2rs} and Q_{2d}, there are essentially andesites ss. These two units correspond to less differentiated rocks of the NHVC.

In general, the NHVC is similar to other volcanoes in the northern Andes with respect to the major elements and trace elements; whether they are LILEs, HFSEs, REEs, or compatible elements, they show behavior representative of orogenic andesites and dacites from the calc–alkaline series with medium K₂O content, which is typical of subduction zones along an active continental margin.

The variations in the chemistry of the mineral phases (plagioclase, clinopyroxene, amphibole, orthopyroxene, olivine, and Fe–Ti oxides) reflect the ranges of formation conditions, with temperatures ranging from 1221 to 710 °C, pressures between 18 and 2 kbar (equivalent to depths between 50 and 3 km), and values of *f*O₂ that indicate oxidizing conditions in magma. The chemical variations also show the complexity in the evolution of the magmas that gave rise to the lavas that participated in the construction of the NHVC.

This complexity in magmatic evolution, sustained also in the isotopic ratios (⁸⁷Sr/⁸⁶Sr and ¹⁴³Nd/¹⁴⁴Nd), is in turn the result of the diversity of processes that participated in the genesis of the magmas that have fed the NHVC. This evolution began with partial melting of the mantle wedge, which allowed enrichment in components derived from the subducting plate. Later, fractional crystallization, probably in an open system, was the main petrogenetic process that controlled magmatic differentiation, although the participation (to a lesser degree) of mechanisms such as crustal contamination and magma mixing cannot be eliminated.

Acknowledgments

We thank the Observatorio Volcanológico y Sismológico de Popayán of the Servicio Geológico Colombiano, the Faculty of Geological Sciences, the Luís Bru Electronic Microscopy Center, and the Isotope Geochronology and Geochemistry Center, which are in the Universidad Complutense de Madrid.

This research was supported in part by the AIBan Scholarship Program of the European Union and by the ICETEX Scholarship Program of Colombia. Thanks to José Luis MACIAS, professor at the Universidad Nacional Autónoma de México, for his support in financing the K–Ar dating performed by Geochron Laboratories (USA). We also thank the geographer Diego PALECHOR, who prepared and edited some of the figures in this chapter. Finally, we extend our thanks to the two reviewers of our manuscript (Julie ROBERGE and John Jairo SÁNCHEZ A.) for their invaluable recommendations.

References

- Alvarado, G., Acevedo, A.P., Monsalve, M.L., Espíndola, J.M., Gómez, D., Hall, M., Naranjo, J.A., Pulgarín, B., Raigosa, J., Sigarán, C. & van der Laat, R. 1999. Desarrollo de la vulcanología en Latinoamérica en el último cuarto del siglo XX. *Revista Geofísica*, 51: 186–241.
- Arcila, M., Muñoz, A. & De Vicente, G. 2000. Marco geotectónico para el noroeste de Suramérica y sur de Centroamérica. *Revista Geotemas*, 1(2): 279–283.
- Ariza, A. 2006. Análisis del retroceso de glaciales tropicales en los Andes centrales de Colombia mediante imágenes Landsat. *Revista Politechnica*, 13(1): 7–23.
- Atherton, M.P. & Petford, N. 1996. Na–rich igneous rocks and crustal thickening in the Andes. *Third Symposium International Géodynamique Andine. Memoirs*, p. 539–542. Saint Malo, France.
- Bailey, J.C. 1981. Geochemical criteria for a refined tectonic discrimination of orogenic andesites. *Chemical Geology*, 32(1–4): 139–154. [https://doi.org/10.1016/0009-2541\(81\)90135-2](https://doi.org/10.1016/0009-2541(81)90135-2)
- Bourdon, E., Eissen, J–P., Monzier, M., Robin, C., Martin, H., Cotten, J. & Hall, M.L. 2002. Adakite–like lavas from Antisana Volcano (Ecuador): Evidence for slab melt metasomatism beneath the Andean Northern Volcanic Zone. *Journal of Petrology*, 43(2): 199–217. <https://doi.org/10.1093/petrology/43.2.199>
- Brizi, E., Molin G. & Zanazzi, P.F. 2000. Experimental study of intracrystalline Fe²⁺–Mg exchange in three augite crystals: Effect of composition on geothermometric calibration. *American Mineralogist*, 85(10):1375–1382. <https://doi.org/10.2138/am-2000-1005>
- Bryant, J.A., Yogodzinski, G.M., Hall, M.L., Lewicki, J.L. & Bailey, D.G. 2006. Geochemical constraints on the origin of volcanic rocks from the Andean Northern Volcanic Zone, Ecuador. *Journal of Petrology*, 47(6): 1147–1175. <https://doi.org/10.1093/petrology/egl006>
- Cardona, C., Santacoloma C., White R., McCausland W., Trujillo N., Narváez A., Bolaños R. & Manzo O. 2009. Sismicidad tipo “DRUMBEAT” asociada a la erupción y emplazamiento de un domo en el Volcán Nevado del Huila, noviembre de 2008. XII Congreso Colombiano de Geología. *Memoirs in CD ROM*, T009–R229. Paipa, Colombia.
- Cardona, C., Manzo, O. & Laverde, C. 2010. Informe de avance sobre el análisis de cambios superficiales asociados a la actividad

- eruptiva en el Volcán Nevado del Huila. Ingeominas, unpublished report, 26 p. Popayán.
- Caro, P. 1995. Geología y geomorfología de la parte central del valle del río Páez entre Irlanda y su confluencia con el río Magdalena. Ingeominas, unpublished report, 79 p. Bogotá.
- Caro, P. & Ruge, G. 1997. Geología, geomorfología y amenazas geológicas en la cuenca del río Páez, Colombia. Ingeominas, unpublished report, 15 p. Bogotá.
- Cas, R.A.F. & Wright, J.V. 1987. Lava flows. In: Cas, R.A.F. & Wright, J.V. (editors), *Volcanic successions: Modern and ancient*. Chapman & Hall, p. 59–92. London.
- Castillo, P.R. 2006. An overview of adakite petrogenesis. *Chinese Science Bulletin*, 51(3): 257–268. <https://doi.org/10.1007/s11434-006-0257-7>
- Cepeda, H. 1987. El vulcanismo moderno en los Andes de Colombia. I Seminario Gerardo Botero Arango sobre la Geología de la Cordillera Central en Colombia. *Memoirs*, p. 1–11. Medellín.
- Cepeda, H., Méndez, R., Murcia, A. & Vergara, H. 1986. Mapa preliminar de riesgos volcánicos potenciales del Nevado del Huila. Scale 1:200 000. Ingeominas, Internal report 1981, 59 p. Medellín.
- Cepeda, H., Murcia, L., Núñez, A. & Parra, E. 1987. Mapa preliminar de amenaza volcánica en Colombia. Scale 1:3 000 000. *Revista CIAF*, 11(1–3): 179–188.
- Cepeda, H., Pulgarín, B. & Correa-Tamayo, A. 1997. The Nevado del Huila Volcanic Complex, Colombia. *International Association of Volcanology and Chemistry of the Earth's Interior General Assembly. Abstracts*, p. 156. Puerto Vallarta.
- Cohen, K.M., Finney, S.C., Gibbard, P.L. & Fan, J.X. 2013 (updated v2020/01). The ICS International Chronostratigraphic Chart. *Episodes*, 36(3): 199–204.
- Cole, J.W., Milner, D.M. & Spinks, K.D. 2005. Calderas and caldera structures: A review. *Earth-Science Reviews*, 69(1–2): 1–26. <https://doi.org/10.1016/j.earscirev.2004.06.004>
- Correa-Tamayo, A.M. 2009. Estudio petrológico, geoquímico y vulcanológico para establecer la evolución magmática del Complejo Volcánico Nevado del Huila, Colombia. Doctoral thesis, Universidad Complutense de Madrid, 353 p. Madrid.
- Correa-Tamayo, A.M. & Ancochea, E. 2015a. Complejo Volcánico Nevado del Huila: Evidencias de su historia eruptiva. *Boletín Geológico*, (43): 41–52. <https://doi.org/10.32685/0120-1425/boletingeo.43.2015.28>
- Correa-Tamayo, A.M. & Ancochea, E. 2015b. Consideraciones geoquímicas y petrogenéticas para establecer la evolución magmática del Complejo Volcánico Nevado del Huila. *Boletín Geológico*, (43): 53–62. <https://doi.org/10.32685/0120-1425/boletingeo.43.2015.29>
- Correa-Tamayo, A.M. & Cepeda, H. 1995. Informe preliminar sobre la geología del Complejo Volcánico Nevado del Huila. Ingeominas, unpublished report, 74 p. Popayán.
- Correa-Tamayo, A.M. & Pulgarín B. 2002. Morfología, estratigrafía y petrografía general del Complejo Volcánico Nevado del Huila (CVNH)—Énfasis en el flanco occidental. Ingeominas, unpublished report, 104 p. Popayán.
- Correa-Tamayo, A.M., Cepeda, H., Pulgarín, B. & Ancochea, E. 2000. El Volcán Nevado del Huila (Colombia): Rasgos generales y caracterización composicional. *Geogaceta*, 27: 51–54.
- Correa-Tamayo, A.M., Ancochea, E. & Pulgarín, B. 2011. Química mineral en las lavas del Complejo Volcánico Nevado del Huila, Colombia. XIII Congreso Colombiano de Geología and XIV Congreso Latinoamericano de Geología. *Memoirs*, p. 387–388. Medellín.
- Deer, W.A., Howie, R.A. & J. Zussman, 1966. *An introduction to the rock-forming minerals*. Longmans, Green and Co. edit., 528 p. London. <https://doi.org/10.1180/DHZ>
- Defant, M.J. & Drummond, M.S. 1990. Derivation of some modern arc magmas by melting of young subducted lithosphere. *Nature*, 347: 662–665. <https://doi.org/10.1038/347662a0>
- de Silva, S.L. & Francis, P.W. 1991. *Volcanoes of the central Andes*. Springer-Verlag, 216 p. Berlin.
- Drummond, M.S. & Defant, M.J. 1990. A model for trondhjemite-tonalite-dacite genesis and crustal growth via slab melting: Archean o modern comparisons. *Journal of Geophysical Research: Solid Earth*, 95(B13): 21503–21521. <https://doi.org/10.1029/JB095iB13p21503>
- Drummond, M.S., Defant, M.J. & Kepezhinskas, P. 1996. Petrogenesis of slab-derived trondhjemite-tonalite-dacite/adakite magmas. *Transactions of the Royal Society of Edinburgh: Earth Sciences*, 87(1–2): 205–215. <https://doi.org/10.1017/S0263593300006611>
- Espinosa, A. 2001. Volcán Nevado del Huila. In: Espinosa, A., *Erupciones históricas de los volcanes colombianos (1500–1995)*. Academia Colombiana de Ciencias Exactas, Físicas y Naturales. Colección Jorge Álvarez Lleras 16, p. 283–287. Bogotá.
- Fabriès, J. 1979. Spinel-olivine geothermometry in peridotites from ultramafic complexes. *Contributions to Mineralogy and Petrology*, 69: 329–336. <https://doi.org/10.1007/BF00372258>
- Flórez, A. 1990. Los nevados de Colombia. *Colombia sus Gentes y Regiones*, 19: 119–126.
- Flórez, A. 1992. Los nevados de Colombia: Glaciales y glaciaciones. *Análisis Geográficos*, 22, 95 p.
- Flórez, A. & Ochoa, F. 1990. El Nevado del Huila o Ñandí. *Colombia sus Gentes y Regiones*, 20: 206–215.
- Forero, J.M. 1956. Volcanes de Colombia. *Boletín de la Sociedad Geográfica de Colombia*, 14(49): 7 p.
- Francis, P. 1993. *Volcanoes, a planetary perspective*. Clarendon Press, 452 p. Oxford.
- Gill, J.B. 1981. *Orogenic andesites and plate tectonics*. Springer-Verlag, 392 p. Berlin. <https://doi.org/10.1007/978-3-642-68012-0>
- Gutscher, M. A., Malavieille, J., Lallemand, S. & Collot, J.Y. 1999. Tectonic segmentation of the North Andean margin: Impact of the Carnegie Ridge collision. *Earth and Planetary Sciences Letters*, 168(3–4): 255–270. [https://doi.org/10.1016/S0012-821X\(99\)00060-6](https://doi.org/10.1016/S0012-821X(99)00060-6)

- Hall, M.L. & Wood, C.A. 1985. Volcano–tectonic segmentation of the northern Andes. *Geology*, 13(3): 203–207. [https://doi.org/10.1130/0091-7613\(1985\)13<203:VSOTNA>2.0.CO;2](https://doi.org/10.1130/0091-7613(1985)13<203:VSOTNA>2.0.CO;2)
- Hantke, G. & Parodi, A. 1966. Catalogue of the active volcanoes of the world, including solfatara fields: Part XIX Colombia, Ecuador and Peru. International Association of Volcanology and Chemistry of the Earth's Interior, 73 p. Rome.
- Helz, R.H. 1973. Phase relations of basalts in their melting range at $P_{H_2O} = 5$ kb as a function of oxygen fugacity: Part I. Mafic phases. *Journal of Petrology*, 14(2): 249–302. <https://doi.org/10.1093/petrology/14.2.249>
- Herd, D.G. 1982. Glacial and volcanic geology of the Ruiz–Tolima Volcanic Complex Cordillera Central, Colombia. *Publicaciones Geológicas Especiales del Ingeominas* 8, 48 p. Bogotá.
- Hubach, E. & Alvarado, B. 1932. Estudios geológicos en la ruta Popayán–Bogotá. Servicio Geológico Nacional, Internal report 213, 132 p. Bogotá.
- Ingeominas. 1995a. Evaluación de amenaza y vigilancia volcánica del Complejo Volcánico Nevado del Huila. Convenio Ingeominas–Corporación Nasa Kiwe, Instituto Colombiano de Geología y Minería (Ingeominas), unpublished report. 27 p. Popayán.
- Ingeominas. 1995b. Zonificación para usos del suelo en la cuenca del río Páez. Convenio Ingeominas–Corporación Nasa Kiwe, unpublished report, 54 p. Popayán.
- Instituto de Hidrología, Meteorología y Estudios Ambientales. 1996. Unidades geomorfológicas del territorio colombiano. 59 p. Bogotá.
- Instituto de Hidrología, Meteorología y Estudios Ambientales. 2017. Glaciares en Colombia. <http://www.ideam.gov.co/web/ecosistemas/glaciares-colombia> (consulted in December 2017).
- Iverson, R.M., Schilling, S.P. & Vallance, J.W. 1998. Objective delineation of lahar–inundation hazard zones. *Geological Society of America Bulletin*, 110(8): 972–984. [https://doi.org/10.1130/0016-7606\(1998\)110<0972:ODOLIH>2.3.CO;2](https://doi.org/10.1130/0016-7606(1998)110<0972:ODOLIH>2.3.CO;2)
- Jaillard, E., Hérail, G., Monfret, T. & Wörner, G. 2002. Andean geodynamics: Main issues and contributions from the 4th ISAG, Göttingen. *Tectonophysics*, 345(1–4): 1–15. [https://doi.org/10.1016/S0040-1951\(01\)00203-7](https://doi.org/10.1016/S0040-1951(01)00203-7)
- James, D.E. & Murcia, L.A. 1984. Crustal contamination in northern Andean volcanics. *Journal of the Geological Society London*, 141: 823–830. <https://doi.org/10.1144/gsjgs.141.5.0823>
- Jiménez, E. 1997. Caracterización sismotectónica del sismo de Páez Cauca 06/06/1994. Bachelor thesis, Universidad Pedagógica y Tecnológica de Colombia, 169 p. Sogamoso.
- Johnson, M.C. & Rutherford, M.J. 1989. Experimental calibration of the aluminum–in–hornblende geobarometer with application to Long Valley caldera (California) volcanic rocks. *Geology*, 17(9): 837–841. [https://doi.org/10.1130/0091-7613\(1989\)017<0837:ECOTAI>2.3.CO;2](https://doi.org/10.1130/0091-7613(1989)017<0837:ECOTAI>2.3.CO;2)
- Kelemen, P.B., Hanghøj, K. & Greene, A.R. 2007. One view of the geochemistry of subduction–related magmatic arcs, with an emphasis on primitive andesite and lower crust. In: Holland, H. & Turekian, K. (editors), *Treatise on Geochemistry*, 3, Elsevier Ltd., p. 1–70. Oxford. <https://doi.org/10.1016/B0-08-043751-6/03035-8>
- Leake, B.E., Woolley, A.R., Arps, C.E.S., Birch, W.D., Gilbert, M.C., Grice, J.D., Hawthorne, E., Kato, A., Kisch, H.J., Krivovichev, V.G., Linthout, K., Laird, J., Mandarino, J., Maresch, W.V., Nickel, E.H., Rock, N.M.S., Schumacher, J.C., Smith, D.C., Stephenson, N.C.N., Ungaretti, L., Whittaker, E.J.W. & Youzhi, G. 1997. Nomenclature of amphiboles Report of the Subcommittee on Amphiboles of the International Mineralogical Association Commission on New Minerals and Mineral Names. *European Journal of Mineralogy*, 9(3): 623–651. <https://doi.org/10.1127/ejm/9/3/0623>
- Leake, B.E., Woolley, A.R., Birch, W.D., Burke, E.A., Ferraris, G., Grice, J., Hawthorne, F.C., Kisch, H.J., Krivovichev, V.G., Schumacher, J.C., Stephenson, N.C.N. & Whittaker, E.J.W. 2004. Nomenclature of amphiboles: Additions and revisions to the International Mineralogical Association's amphibole nomenclature. *Mineralogical Magazine*, 68(1): 209–215. <https://doi.org/10.1180/0026461046810182>
- Le Maitre, R.W. 1976. Some problems of the projection of chemical data into mineralogical classifications. *Contributions to Mineralogy and Petrology*, 56(2): 181–189. <https://doi.org/10.1007/BF00399603>
- Lepage, L.D. 2003. ILMAT: An Excel worksheet for ilmenite–magnetite geothermometry and geobarometry. *Computers & Geosciences*, 29(5): 673–678. [https://doi.org/10.1016/S0098-3004\(03\)00042-6](https://doi.org/10.1016/S0098-3004(03)00042-6)
- Londoño, J.M. & Cardona, C.E. 2011. Sismicidad asociada a la reactivación del Volcán Nevado del Huila: Un modelo de actividad sísmica. XIV Congreso Latinoamericano de Geología and XIII Congreso Colombiano de Geología. *Memoirs*, p. 386–387. Medellín.
- Manzo, O.H., Santacoloma, C.C. & Laverde, C.A. 2011. Análisis de cambios superficiales asociados a la actividad eruptiva en el Volcán Nevado del Huila entre 2007 y 2010. XIV Congreso Latinoamericano de Geología and XIII Congreso Colombiano de Geología. *Memoirs*, p. 209–210. Medellín.
- Marín–Cerón, M. 2007. Major, trace element and multi–isotopic systematics of SW Colombian volcanic arc, northern Andes: Implication for the stability of carbonate rich sediment at subduction zone and the genesis of andesite magma. Doctoral thesis, Okayama University, 139 p. Okayama, Japan.
- Martin, H. 1986. Effect of steeper Archean geothermal gradient on geochemistry of subduction–zone magmas. *Geology*, 14(9): 753–756. [https://doi.org/10.1130/0091-7613\(1986\)14<753:EOSAGG>2.0.CO;2](https://doi.org/10.1130/0091-7613(1986)14<753:EOSAGG>2.0.CO;2)
- Martin, H. 1999. Adakitic magmas: Modern analogues of Archaean granitoids. *Lithos*, 46(3): 411–429. [https://doi.org/10.1016/S0024-4937\(98\)00076-0](https://doi.org/10.1016/S0024-4937(98)00076-0)

- Maury, R.C., Sajona, F.G., Pubellier, M., Bellon, H. & Defant, M.J. 1996. Fusion de la croûte océanique dans les zones de subduction-collision récentes: L'exemple de Mindanao (Philippines). *Bulletin de la Société Géologique de France*, 167 (5): 579–595.
- Meissner, R., Fliih, E. & Muckelmann, R. 1980. Sobre la estructura de los Andes septentrionales—Resultados de investigaciones geofísicas. In: Nuevos resultados de la investigación geocientífica en Latinoamérica. Deutsche Forschungsgemeinschaft, p. 79–90. Bonn.
- Monsalve, M.L., Pulgarín, B., Mojica, J., Santacoloma, C.C. & Cardona, C.E. 2011. Interpretación de la actividad eruptiva del Volcán Nevado del Huila (Colombia), 2007–2009: Análisis de componentes de materiales emitidos. *Boletín de Geología*, (33)2: 73–93. Bucaramanga.
- Morimoto, N., Fabries, J., Ferguson, A.K., Ginzburg, I.V., Ross, M., Seifert, F.A., Zussman, J., Aoki, K. & Gottardi, G. 1988. Nomenclature of pyroxenes. *Mineralogical Magazine*, 52(367): 535–550. <https://doi.org/10.1180/minmag.1988.052.367.15>
- Nakamura, N. 1974. Determination of REE, Ba, Fe, Mg, Na and K in carbonaceous and ordinary chondrites. *Geochimica et Cosmochimica Acta*, 38(5): 757–775. [https://doi.org/10.1016/0016-7037\(74\)90149-5](https://doi.org/10.1016/0016-7037(74)90149-5)
- Orrego, A. 1982. Geología y geoquímica del área mineralizada El Pisco, Silvia. (Cauca, Colombia). *Publicaciones Geológicas Especiales del Ingeominas*, 10: 47–63. Bogotá.
- Orrego, A. & París, G. 1991. Cuadrángulo N–6, Popayán: Geología, geoquímica y ocurrencias minerales. *Ingeominas, Internal report 2160*, 181 p. Popayán.
- Otten, M.T. 1984. The origin of brown hornblende in the Artfjället gabbro and dolerites. *Contributions to Mineralogy and Petrology*, 86: 189–199. <https://doi.org/10.1007/BF00381846>
- Pearce, J.A. 1983. Role of the sub–continental lithosphere in magma genesis at active continental margins. In: Hawkesworth, C.J. & Norry, M.J. (editors), *Continental basalts and mantle xenoliths*. Shiva Publications, p. 230–249. Nantwich, UK.
- Pennington, W.D. 1981. Subduction of the eastern Panama Basin and seismotectonics of northwestern South America. *Journal of Geophysical Research: Solid Earth*, 86(B11): 10753–10770. <https://doi.org/10.1029/JB086iB11p10753>
- Powell, R. & Powell M. 1977. Geothermometry and oxygen barometry using coexisting iron–titanium oxides: A reappraisal. *Mineralogical Magazine*, 41(318): 257–263. <https://doi.org/10.1180/minmag.1977.041.318.14>
- Pulgarín, B. 2000. Depósitos masivos del Pleistoceno tardío, asociados al colapso del flanco sur del Volcán Nevado del Huila (Colombia). Master thesis, Universidad Nacional Autónoma de México, 135 p. México D.F.
- Pulgarín, B. 2003. Mapa de amenaza por un flujo de escombros de gran volumen, simulado sobre el valle del río Páez. IX Congreso Colombiano de Geología. Abstracts, p. 143–144. Medellín.
- Pulgarín, B. 2012. Informe de la primera visita técnica al domo nuevo del Volcán Nevado del Huila. Servicio Geológico Colombiano, unpublished report, 52 p. Popayán.
- Pulgarín, B. & Correa–Tamayo, A.M. 1997. Depósitos fragmentarios no consolidados sobre el edificio del Complejo Volcánico Nevado del Huila. *Ingeominas*, unpublished report, 55 p. Popayán.
- Pulgarín, B. & Correa–Tamayo, A.M. 2001. Depósitos fragmentarios no consolidados sobre el edificio del Complejo Volcánico Nevado del Huila (CVNH): Relación con los sistemas morfogénicos de alta montaña, clasificación y caracterización. VIII Congreso Colombiano de Geología and V Conferencia Colombiana de Geología Ambiental. *Memoirs in CD ROM*, 15 p. Manizales.
- Pulgarín, B. & Correa–Tamayo, A.M. 2003. Morrenas del Volcán Nevado del Huila y su correlación con otras áreas glaciadas de Colombia. IX Congreso Colombiano de Geología. Abstracts, p. 151. Medellín.
- Pulgarín, B. & Laverde, C. 2015a. Análisis de densidad de cenizas del ciclo eruptivo 2007–2010 en el Volcán Nevado del Huila. XV Congreso Colombiano de Geología. *Memoirs*, p. 794–800. Bucaramanga.
- Pulgarín, B. & Laverde, C. 2015b. Actualización del mapa de amenaza volcánica por caída de piroclastos del Volcán Nevado del Huila. XV Congreso Colombiano de Geología. *Memoirs*, p. 783–789. Bucaramanga.
- Pulgarín, B., Jordan, E. & Linder, W. 1996. Nevado del Huila (Colombia): Cambio glaciar entre 1961 y 1995. VII Congreso Colombiano de Geología, IV Conferencia Colombiana de Geología Ambiental and II Seminario sobre el Cuaternario en Colombia. *Memoirs*, I, p. 441–451. Bogotá.
- Pulgarín, B., Cepeda, H. & Correa–Tamayo, A.M. 1997a. Unidades geológicas y geomorfológicas de Colombia: Formación Nevado del Huila. *Ingeominas*, unpublished report, 15 p. Popayán.
- Pulgarín, B., Cepeda, H. & Correa–Tamayo, A.M. 1997b. Geología del Complejo Volcánico Nevado del Huila. *Ingeominas*, unpublished report, 32 p. Popayán.
- Pulgarín, B., Macías, J.L., Cepeda, H. & Capra L. 2004. Late Pleistocene deposits associated with a southern flank collapse of the Nevado del Huila Volcanic Complex (Colombia). *Acta Vulcanologica* 16(1–2): 37–58. Roma.
- Pulgarín, B., Jordan, E. & Linder, W. 2007. Aspectos geológicos y cambio glaciar del Nevado del Huila entre 1961 y 1995. Primera Conferencia Internacional de Cambio Climático: Impacto en los sistemas de alta montaña. *Memoirs*, p. 123–140. Bogotá.
- Pulgarín, B., Cardona, C.E., Santacoloma, C., Agudelo, A., Calvache, M.L. & Monsalve, M.L. 2008. Erupciones del Volcán Nevado del Huila, en febrero y abril de 2007, y los cambios en su masa glaciar. *Boletín Geológico*, 42(1–2):109–127. <https://doi.org/10.32685/0120-1425/boletingeo.42.2008.23>
- Pulgarín, B., Cardona, C., Agudelo, A., Santacoloma, C., Monsalve, M., Calvache, M., Murcia, H., Ibáñez, D., García, J., Murcia, C., Cuellar, M., Ordóñez, M., Medina, E., Balanta, R.,

- Calderón, Y. & Leiva, O. 2009. Erupciones históricas recientes del Volcán Nevado del Huila, cambios morfológicos y lahares asociados. XII Congreso Colombiano de Geología. Digital abstracts, CD ROM T009–R287. Paipa, Colombia.
- Pulgarín, B., Laverde, C., Manzo, O., Valencia, G. & Galarza, J. 2014. 1961–2013 variation of the glacial area at Nevado del Huila Volcano (Colombia), and effects on the glacier due to the eruptive activity between 2007 and 2010. In: Ifrim, C., Cueto, F.J. & Stinnesbeck, W. (editors), 23rd Latin American Colloquium on Earth Sciences. Abstracts and Programme. GAEA heidelbergensis 19, Poster 020, p. 130. Heidelberg, Germany.
- Pulgarín, B., Cardona, C., Agudelo, A., Santacoloma, C., Monsalve, M.L., Calvache, M., Murcia, C., Cuéllar, M., Medina, E., Balanta, R., Calderón, Y., Leiva, Ó., Ordóñez, M. & Ibáñez, D. 2015. Erupciones recientes del Volcán Nevado del Huila: Lahares asociados y cambios morfológicos del glaciar. *Boletín Geológico*, 43: 75–87. Bogotá. <https://doi.org/10.32685/0120-1425/boletingeo.43.2015.21>
- Putirka, K.D. 2005. Cpx–Plag–Ol Thermobar Workbook. http://www.fresnostate.edu/csm/ees/documents/facstaff/putirka/Use_of_Workbook.pdf
- Putirka, K.D. 2008. Thermometers and barometers for volcanic systems. *Reviews in Mineralogy and Geochemistry*, 69 (1): 61–120. <https://doi.org/10.2138/rmg.2008.69.3>
- Ramírez, J.E. 1968. Los volcanes de Colombia. *Revista de la Academia Colombiana de Ciencias Exactas, Físicas y Naturales*, 13(50): 227–234.
- Rollinson, H.R. 1993. Using geochemical data: Evaluation, presentation, interpretation. Longman Group UK Limited, 352 p. Harlow, UK.
- Rudnick, R.L. & Gao, S. 2003. Composition of the continental crust. In: Holland, H.D. & Turekian, K.K. (editors), *Treatise on Geochemistry*, 3. Elsevier Ltd., p. 1–64. Oxford. <https://doi.org/10.1016/B0-08-043751-6/03016-4>
- Samaniego, P., Martin, H., Monzier, M., Robin, C., Fornari, M., Eisen, J.P. & Cotten, J. 2005. Temporal evolution of magmatism in the Northern Volcanic Zone of the Andes: The geology and petrology of Cayambe Volcanic Complex (Ecuador). *Journal of Petrology*, 46(11): 2225–2252. <https://doi.org/10.1093/ptrology/egi053>
- Santacoloma, C., Cardona, C.E., White, R., McCausland, W., Trujillo, N., Bolaños, R., Manzo, O. & Narváez, A. 2009. Aspectos sísmicos de las erupciones freáticas y freatomagmáticas del Volcán Nevado del Huila (Colombia). XII Congreso Colombiano de Geología. Digital abstracts, CD ROM T009–R223. Paipa, Colombia.
- Short, N.M. 1986. Volcanic landforms. In: Short, N.M. & Blair Jr., R.W. (editors), *Geomorphology from space: A global overview of regional landforms*. NASA Special Publication 486. 709 p. Washington. http://geoinfo.amu.edu.pl/wpk/geos/GEO_3/GEO_CHAPTER_3_TABLE.HTML
- Simkin, T. 1981. *Volcanoes of the world*. Smithsonian Institution. Hutchinson Ross Publishing. Co. 232 p. New York.
- Soto, J.I. & Soto, V.M. 1995. PTMAFIC: Software package for thermometry, barometry, and activity calculations in mafic rocks using an IBM-compatible computer. *Computers & Geosciences*, 21(5): 619–652. [https://doi.org/10.1016/0098-3004\(94\)00101-Y](https://doi.org/10.1016/0098-3004(94)00101-Y)
- Stormer Jr., J.C. & Nicholls, J. 1978. XLFRAC: A program for the interactive testing of magmatic differentiation models. *Computers & Geosciences*, 4(2): 143–159. [https://doi.org/10.1016/0098-3004\(78\)90083-3](https://doi.org/10.1016/0098-3004(78)90083-3)
- Stübel, A. 1906. *Die Vulkanberge von Colombia: Geologisch–Topographisch Aufgenommen und Beschrieben*. Verlag von Wilhelm Baensch. 154 p. Dresden, Germany.
- Sun, S. & McDonough, W.F. 1989. Chemical and isotopic systematics of oceanic basalts: Implications for mantle composition and processes. In: Saunders, A. & Norry, M.J. (editors), *Magmatism in the ocean basins*. Geological Society of London, Special Publication 42, p. 313–345. <https://doi.org/10.1144/GSL.SP.1989.042.01.19>
- Taboada, A., Rivera, L., Fuenzalida, A., Cisternas, A., Philip, H., Bijwaard, H., Olaya, J. & Rivera, C. 2000. Geodynamics of the northern Andes: Subductions and intracontinental deformation (Colombia). *Tectonics*, 19(5): 787–813. <https://doi.org/10.1029/2000TC900004>
- Thorpe, R.S., Francis, W.W. & O’Callaghan, L. 1984. Relative roles of source composition, fractional crystallization and crustal contamination in the petrogenesis of Andean volcanic rocks. *Philosophical Transactions of the Royal Society of London, A, Mathematical, Physical and Engineering Sciences*, 310(1514): 675–692. <https://doi.org/10.1098/rsta.1984.0014>
- Tischendorf, G., Förster, H.J. & Gottesmann, B. 2001. Minor- and trace-element composition of trioctahedral micas: A review. *Mineralogical Magazine*, 65(2): 249–276. <https://doi.org/10.1180/002646101550244>
- Toussaint, J. & Restrepo, J. 1991. El magmatismo en el marco de la evolución geotectónica de Colombia. Simposio sobre Magmatismo Andino y su Marco Tectónico. Abstracts, p. 44. Manizales.
- van der Hammen, T. 1981. Glaciales y glaciaciones en el Cuaternario de Colombia. *Paleoecología y Estratigrafía*. *Revista CIAF*, 6 (1–3): 635–638.
- van der Wiel, A.M. 1991. The volcanoclastic terraces along the río Páez and downstream part of the río La Plata. In: van der Wiel, A.M. *Uplift and volcanism of the SE Colombian Andes in relation to Neogene sedimentation in the Upper Magdalena Valley*. Doctoral thesis, Agricultural University, p. 169–181. Wageningen, The Netherlands.
- van Zuidam, R.A. 1986. Aerial photo-interpretation in terrain analysis and geomorphologic mapping. *International Institute for Aerospace Survey and Earth Sciences*, 442 p. The Netherlands.

Explanation of Acronyms, Abbreviations, and Symbols:

Ab	Albite	MORB	Mid-ocean ridge basalts
AD	Anno Domini	MREEs	Middle rare earth elements
AHS	Ancient Huila Stage	Mt	Magnetite
Am	Amphibole	NHVC	Nevado del Huila Volcanic Complex
An	Anorthite	NVZ	North Volcanic Zone
Ann	Annite	OIB	Oceanic island basalts
AVZ	Austral Volcanic Zone	OI	Olivine
BP	Before the present	Op	Opaques
Bt	Biotite	Opx	Orthopyroxene
cf.	Confer, compare	Or	Orthoclase
Chr	Chromite	PASP	Phlogopite–annite / siderophyllite –polyolithionite
Cpx	Clinopyroxene	Phl	Phlogopite
CVZ	Central Volcanic Zone	PHS	Pre–Huila Stage
En	Enstatite	Plag	Plagioclase
EPMA	Electron probe microanalyzer	Ple	Pleonaste
Fo	Forsterite	PNNP	Parque Nacional Natural Los Nevados
Fs	Ferrosilite	QFM	Quartz–fayalite–magnetite
Hem	Hematite	REEs	Rare earth elements
HFSEs	High field strength elements	RHS	Recent Huila Stage
HM	Hematite–magnetite	ss	Sensu stricto
HREEs	Heavy rare earth elements	SVZ	South Volcanic Zone
ICP	Inductively coupled plasma	TAS	Total alkali silica
ICP–MS	Inductively coupled plasma mass spectrometry	TIMS	Thermal ionization mass spectrometer
Ilm	Ilmenite	Usp	Ulvospinel
LILEs	Large ion lithophile elements	WDS	Wavelength dispersive spectroscopy
LREEs	Light rare earth elements	Wo	Wollastonite

Authors' Biographical Notes



Ana María CORREA-TAMAYO is a geologist (1992) with a PhD in geology (2009) from the Universidad Complutense de Madrid. Her professional job has been focused on volcanic cartography and stratigraphy, petrographic and geochemical studies of volcanoes, and their eruptive history. She has been working at the Servicio Geológico Colombiano (SGC) for 10 years. She has

performed geological work and research on several Colombian volcanoes (Nevado del Huila, Azufral, Paramillo de Santa Rosa, Doña Juana, Nevado del Ruiz, and Sotará). She is currently a member of the Grupo de Geología de Volcanes of the SGC.



Bernardo Alonso PULGARÍN-ALZATE is a geologist engineer (1987) with an MS in volcanology (2000) from the Universidad Nacional Autónoma de México. His professional job has been focused on understanding volcanic geology–stratigraphy and the eruptive histories of volcanoes as well as in the searching for good practices for standardization of volcanoes geological

maps. He also has experience working with volcanic hazards, glacier retreat, and socialization and communication with communities that live under threat of geological hazards. He has worked for the Servicio Geológico Colombiano (SGC) at the Observatorio Vulcanológico y Sismológico de Popayán for 32 years. He has carried out geological work and research on several Colombian volcanoes (Puracé, Los Co-

conucos volcanic chain, Nevado de Santa Isabel, Nevado del Huila, Doña Juana, Sotar, Sucubn, Nevado del Ruiz, Paramillo de Santa Rosa, and Galeras). He is currently the coordinator of the Grupo de Geologa de Volcanes of the SGC.



Eumenio ANCOCHEA-SOTO bachelor of geological sciences and PhD (1982) in geological sciences from the Universidad Complutense de Madrid. Extraordinary Degree and Doctorate award. Since 1976, he has been a professor at the Universidad Complutense de Madrid, mainly in the areas of petrology and geochemistry. His research has always been linked to volcanism for more than 30 years, in

aspects such as volcano-stratigraphy, isotopic geochronology, paleo-volcanism, origin of magmas, regional volcanology, volcanic risk, and growth and evolution of large structures and volcanic edifices. He has performed geological work and research in different volcanic areas: the Central Spanish Volcanic Region, Canary Islands, Cape Verde, Colombia, and Morocco. He has been the secretary and director of the Department of Petrology and Geochemistry, vice-dean of Studies of the Faculty of Geological Sciences, dean of the same (1994–2011), and vice-chancellor of Academic Organization. He is the director of the “Volcanism Research Group” of the Universidad Complutense de Madrid. He has been the principal investigator on numerous research projects. Other outstanding positions include member and vice president of the Volcanology Section of the Spanish Commission of Geodesy and Geophysics and Corresponding Academician of the Royal Academy of Physical, Exact and Natural Sciences since 1999.

